Coordination Chemistry Reviews 254 (2010) 2603–2622

Contents lists available at ScienceDirect

Coordination Chemistry Reviews

journal homepage: www.elsevier.com/locate/ccr

Review

Design of luminescent iridium(III) and rhenium(I) polypyridine complexes as *in vitro* and *in vivo* ion, molecular and biological probes

Kenneth Kam-Wing Lo*, Man-Wai Louie, Kenneth Yin Zhang

Department of Biology and Chemistry, City University of Hong Kong, Tat Chee Avenue, Kowloon, Hong Kong, China

Contents

ARTICLE INFO

Article history:
Received 30 October 2009
Accepted 26 January 2010
Available online 2 February 2010

Keywords:
Iridium
Luminescence
Probes
Rhenium

ABSTRACT

Many luminescent transition metal polypyridine complexes display intense and long-lived triplet charge-transfer and intraligand transition emission with a large Stokes' shift. These properties render them promising candidates as luminescent probes for ions, DNA, peptides, proteins and other biological entities. In this review article, we have summarised recent reports on ion, molecular and biological probes derived from luminescent rhenium(I) and iridium(III) polypyridine complexes. These complexes have been appended with different recognition moieties that interact with ions and biological molecules. The recognition is reflected by a change of spectroscopic and/or photophysical properties of the probes. The use of these complexes as cellular probes and imaging reagents has also been discussed.

Abbreviations: bpy, 2,2′-bipyridine; BSA, bovine serum albumin; β-CD, β-cyclodextrin; CM, coumarin; CT, charge-transfer; DPB, 4,4′-dipyridylbutadiyne; dpp[5], 1,5-bis(4-pyridyl)pentane; dppn, benzo[*i*]dipyrido[3,2-*a*:2′,3′-*c*]phenazine; dppz, dipyrido[3,2-*a*:2′,3′-*c*]phenazine; dpq, dipyrido[3,2-*f*:2′,3′-*h*]quinoxaline; dpqa, 2-*n*-butylamidodipyrido[3,2-*f*:2′,3′-*h*]quinoxaline; DSPC, 1,2-distearoyl-*sn*-glycero-3-phosphocholine; en, ethylenediamine; ERα, estrogen receptor α; FIrpic, bis(4,6-difluorophenylpyridinato-*N*,C_2)picolinatoiridium; FRET, fluorescence resonance-energy transfer; HABA, 4′-hydroxyazobenzene-2-carboxylic acid; Hacac, acetylacetone; HSA, human serum albumin; HBpq, 2-(4-(dimesitylboryl)phenyl)quinoline; Hbsb, 2-((1,1′-biphenyl)-4-yl)benzothiazole; Hbsn, 2-(1-naphthyl)benzothiazole; Hbt, 2-phenylbenzothiazole; Hbtth, 2-(2-thienyl)benzothiazole; Hbzq, 7,8-benzoquinoline; Hmppy, 2-(4-methylphenyl)pyridine; Hmppz, 3-methyl-1-phenylpyrazole; Hpba, 4-(2-pyridyl)benzaldehyde; Hppy, 2-phenylpyridine; Hppz, 1-phenylpyrazole; Hpq, 2-phenylquinoline; IgG, immunoglobulin G; IL, intraligand; MC, metal-centred; MeA, adamantanemethyl; mCP, *N*,*N*′-dicarbazolyl-3,5-benzene; MLCT, metal-to-ligand charge-transfer; MPO, 2-mercaptopyridine-*N*-oxide; MTT, 3-(4,5-dimethyl-2-thiazolyl)-2,5-diphenyltetrazolium bromide; PBS, phosphate buffered saline; PE, dipalmitoyl-L-α-phosphatidylethanolamine; phen, 1,10-phenanthroline; phi, phenanthrene-9,10-diimine; PMC, *N*-(2-pyridinylmethylene)-2,3,5,6,8,9,11,12-octahydro-1,4,7,10,13-benzopentaoxacyclononadecan-16-ylamine; py, pyridine; py-az, 1-(4-pyridinylformyl)aza-15-crown-5; py-biotin-NCS, 3-isothiocyanato-5-((2-(biotinamido)ethyl)aminocarbonyl)pyridine; py-biotin-TU-Et, 3-ethylthioureidyl-5-((2-(biotinamido)ethyl)aminocarbonyl)pyridine; py-C6-est, 4-(*N*-(6-(4-(17α-ethynylestradiolyl)benzoylamino)hexanoyl)aminomethyl)pyridine; py-TU-DPAT, 3-(2-(4-hydroxy-3-(2,2′-dipicolylaminomethyl)phenyl)ethylthioureidyl)pyridine; py-TU-Et, 3-(ethylthioureidyl)pyridine; quqo, 2-(quinolin-2-yl)quinoxaline; RET, resonance-energy transfer; r-SAv, recombinant streptavidin; SAv, streptavidin; SCE, saturated calomel electrode; TBAH, tetra-*n*-butylammonium hexafluorophosphate; TDDFT, time-dependent density functional theory; tpm, tris(1-pyrazolyl)methane; tpy, 2,2′:6′,2″-terpyridine; ttpy, 4′-tolyl-2,2′:6′,2″-terpyridine; TU, thiourea.

* Corresponding author. Tel.: +852 2788 7231; fax: +852 2788 7406.
E-mail address: bhkenlo@cityu.edu.hk (K.K.-W. Lo).

0010-8545/$ – see front matter © 2010 Elsevier B.V. All rights reserved.
doi:10.1016/j.ccr.2010.01.014

1. Introduction

The spectroscopic, photophysical and photochemical properties of rhenium(I) polypyridine complexes have been attracting much interest for more than 30 years [1–6]. Rhenium(I) polypyridine complexes, $[Re(N^N)(CO)_3(L)]$ (L = monodentate ligands such as halide, pyridines, phosphines and alkyls), exhibit long-lived and intense emission at room temperature upon photoexcitation. The emission energies of these complexes depend heavily on the π^* orbital of the polypyridine ligand, and the emission lifetimes and quantum yields are also very sensitive to the solvent polarity. Based on the photophysical data, the excited state of these complexes has been ascribed to ^{3}MLCT ($d\pi(Re) \rightarrow \pi^*(N^N)$) in nature. In some cases, however, the emissive state is ^{3}IL ($\pi \rightarrow \pi^*(N^N)$) in character [7]. The relative dominance of MLCT and IL emission can be controlled by the energetic separation of the ^{3}MLCT and ^{3}IL states, which can be manipulated by changing the polypyridine ligands or temperature. Since the first report on the luminescence properties of rhenium(I) polypyridine systems [1], the environment-sensitive emission, photoinduced electron-transfer and photocatalytic properties of these complexes have been extensively studied. One of the important characteristics of luminescent rhenium(I) polypyridine complexes is that their emission maxima exhibit blue shifts in rigid media [2]. The emission energies, quantum yields and lifetimes of the complexes decrease with increasing polarity of solvents [1–7]. This highly environment-sensitive luminescence behaviour renders this class of complexes useful biological probes. Functionalisation of these luminescent complexes as cellular-staining reagents has been studied owing to their intense and long-lived emission, high cellular uptake efficiency, and their stability in aqueous condition.

The luminescence properties of iridium(III) polypyridine complexes have been attracting much attention since the emissive characteristics of the complex *cis*-$[Ir(bpy)_2Cl_2]^+$ were studied [8]. The two emission bands of this complex are assigned to excited states of ^{3}MC ($d\pi(Ir) \rightarrow d\sigma^*(Ir)$) and mixed ^{3}MLCT ($d\pi(Ir) \rightarrow \pi^*(bpy)$) and ^{3}IL ($\pi \rightarrow \pi^*$)(bpy) character. The dichloro-bridged iridium(III) dimer $[Ir_2(N^C)_4Cl_2]$ reacts with various ligands to form strongly emitting complexes. For example, a number of cyclometallated iridium(III) polypyridine complexes of the formula $[Ir(N^C)_2(N^N)]^+$ exhibit intense and long-lived ^{3}MLCT ($d\pi(Ir) \rightarrow \pi^*(N^N$ or $N^C)$) and/or ^{3}IL ($\pi \rightarrow \pi^*(N^N$ or $N^C)$) emission in the visible region [9,10], which enables them to function as luminescent sensors for a range of ions and molecules.

In this review, we have described the design of luminescent rhenium(I) and iridium(III) polypyridine complexes as probes for ions, small molecules and biomolecules such as DNA and proteins. Emphasis has been put on the structures, spectroscopic properties, emission properties and molecular binding properties of the complexes. Additionally, we have summarised recent studies of the cellular uptake characteristics and cytotoxicity of these complexes.

2. Rhenium(I) complexes

2.1. Ion and small molecule probes

Rhenium(I) polypyridine complexes functionalised with a crown pendant $[Re(PMC)(CO)_3Cl]$ (**1**) and $[Re(phen)(CO)_3(py\text{-}az)]^+$ (**2**) have been synthesised [11]. Addition of alkali metal or alkaline earth metal ions to a methanolic solution of complex **1** results in a blue shift of the ^{1}MLCT/^{1}IL admixture absorption band from 410 to 375 nm. This shift is ascribed to the binding of the cations to the crown ether cavity since similar effect is not observed for the crown-free complex. Among the cations studied, sodium ion gives the largest stability constant, with a log K value of 2.55. In the case of potassium ion, two adducts with binding stoichiometries (K^+:Re) of 1:2 and 1:1 are formed. Upon photoexcitation, all the complexes exhibit intense and long-lived yellow-green to orange-red ^{3}MLCT emission. Addition of ions results in changes of the emission properties of the crown ether complexes, rendering them sensitive ion sensors.

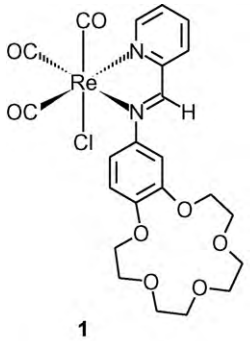

1

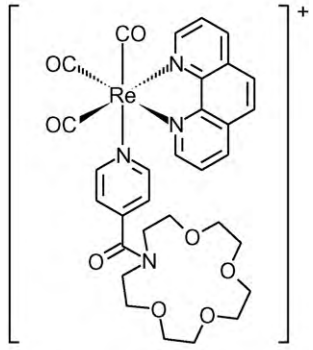

2

Sullivan and co-worker developed luminescent rhenium(I) 5-substituted-1,10-phenanthroline complex [Re(phen-5-aza-18-crown-6)$(CO)_3$Cl] (**3**) [12]. The addition of an amino substituent to the phenanthroline ligand allows the complex to function as a luminescent metal ion sensor. Treatment of the complex with $Pb(OAc)_2$ in MeOH under moderate 15-fold excess conditions leads to a ca. 20-nm red shift and a 2.7-fold increase in emission intensity. A similar reaction with $Ba(OAc)_2$ under 50-fold excess conditions leads to a 10-nm red shift and only a 25% increase in emission intensity.

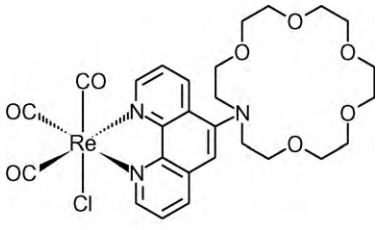

3

Lees and co-worker reported a luminescent dinuclear rhenium(I) polypyridine complex [{Re(^{t}Bu$_2$-bpy)$(CO)_3$}$_2${(py-

NHCO)$_2$py}]$^{2+}$ (**4**) [13]. In degassed CH_2Cl_2, the complex exhibits intense absorption bands in the near UV to visible spectral region (λ_{max} = 254–380 nm) and a very strong emission band at 536 nm (Φ_{em} = 0.37, τ_o = 0.48 μs) upon excitation. Addition of halides or inorganic polyatomic anions into a CH_2Cl_2 solution of the complex results in emission quenching with a concomitant red shift of the emission wavelength from 536 to 546 nm. The binding stoichiometry is 1:1. This complex shows strong binding affinity towards halide, cyanide and acetate ions, but only moderate binding towards dihydrogen phosphate and very weak binding strengths to nitrate and perchlorate ions. Importantly, the sensitivity of the complex is so high that the emission intensity is effectively quenched by as much as 10% even in the presence of only 10^{-8} M cyanide or fluoride ion.

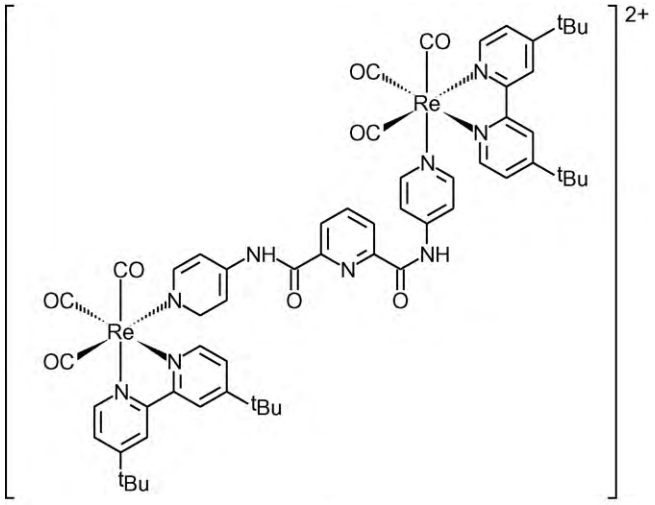

4

Rhenium(I) bipyridine complexes appended with a fluorescent coumarin unit via an oligoether spacer, [Re(bpy)(CO)$_3$(py-O$_n$-CM)]$^+$ (n = 3–6) (**5**) and [Re(bpy-CM)(CO)$_3$(py)]$^+$ (**6**), have been synthesised and characterised by Yam and co-workers [14]. These complexes exhibit strong yellow luminescence upon excitation in CH_3CN at room temperature. In addition to the intense ^{3}MLCT emission band at ca. 570 nm, the complexes also exhibit a weaker emission band at ca. 420 nm, which is assigned to the fluorescence of coumarin. The relatively weak coumarin emission is attributed to FRET from this organic unit to the rhenium bipyridine moiety. This energy transfer efficiency can be perturbed upon addition of selected metal ions; for example, the presence of Mg^{2+} ion in a CH_3CN solution of [Re(bpy)(CO)$_3$(py-O$_5$-CM)]$^+$ leads to a large increase in the coumarin donor fluorescence intensity at ca. 422 nm, and a drop in the emission intensity of the rhenium(I) polypyridine unit at ca. 570 nm. Similar changes are also observed in the case of Ca^{2+} and Pb^{2+} ions, except that the emission spectral changes are not as large as that of Mg^{2+} ion. It is likely that the binding of the smaller metal ion results in the conformational changes of the molecule, which in turn increases the donor–acceptor separation and hence reduces the FRET efficiency. Interestingly, upon addition of Ba^{2+} ion, the emission intensities of both the donor and the acceptor are slightly increased. This unexpected observation originates from rigidification of the molecule upon the ion-binding event.

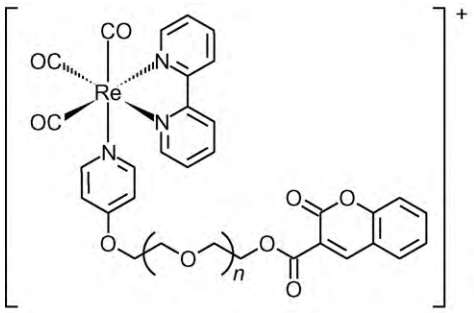

5

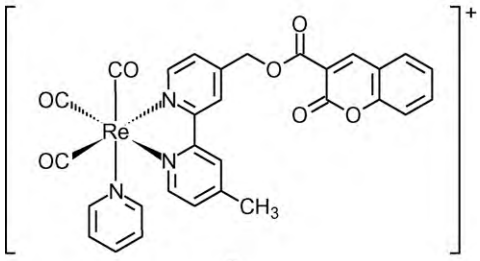

6

Beer and co-workers prepared a series of novel rhenium(I) bipyridine complexes such as (**7**) that contains both a crown ether pendant and an amide unit [15]. The photophysical and ion-pair-binding properties have been examined. Emission titrations show that the emission intensities of the complexes are enhanced and the emission bands are blue-shifted in the presence of tetrabutylammonium acetate or chloride. The emission enhancement is ascribed to the increase of rigidity of the complexes, which inhibits collisional deactivation, upon ion binding. The binding constants (log K) of the complexes for these two ions are 4.00–5.04. Interestingly, in the presence of K^+, these values increase to 4.18 and 5.89, respectively, implying that the presence of bound potassium ion has a positive cooperative effect on the anion-binding properties of the complexes.

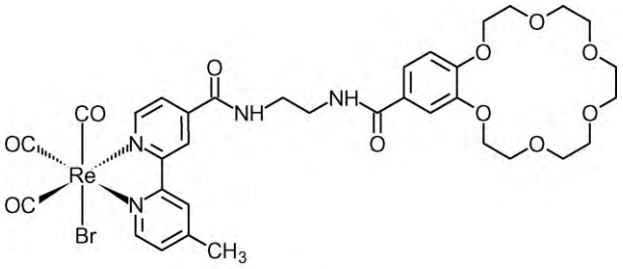

7

Sun and Lees isolated a series of self-assembled macrocyclic compounds featuring [Re(CO)$_3$X] (X = Cl or Br) as corners and linear bipyridine bridging ligands [16]. The photophysical properties of the complexes have been investigated. Both the square [Re(μ-DPB)(CO)$_3$Cl]$_4$ (**8a**) and the corner [Re(DPB)$_2$(CO)$_3$Br] (**8b**) complexes show excellent sensing properties towards nitro-substituted aromatic compounds. In THF, the emission of both complexes is effectively quenched by these compounds with quenching rate constants ranging from 4.94×10^8 to 9.12×10^9 M^{-1} s^{-1}. The emission bands of both complexes in solid films occur at higher energy compared to those in solution. While

the solid film of $[Re(\mu\text{-DPB})(CO)_3Cl]_4$ displays significant emission quenching after exposure to 2,3-dinitrotoluene vapour for 180 s, $[Re(DPB)_2(CO)_3Br]$ does not give a similar observation. The quenching effect occurring in the film of $[Re(\mu\text{-DPB})(CO)_3Cl]_4$ is apparently due to its porosity, which provides cavities for binding the quencher molecules.

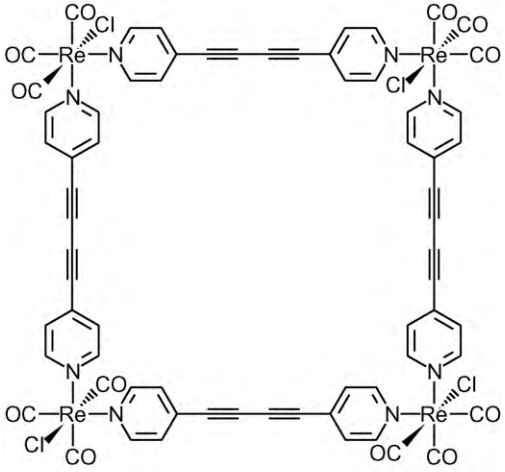

8a

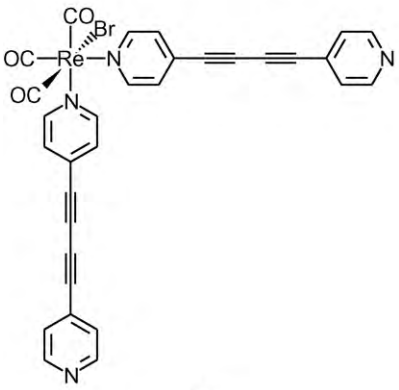

8b

2.2. DNA probes

Schanze and Yam studied, respectively, the luminescence properties of the complexes, $[Re(N^N)(CO)_3(L)]^+$ (N^N = dppz, dppn; L = py, py-4-Me) (**9**) with an extended planar diimine ligand [17–19]. Luminescence and transient absorption spectroscopy shows that the dppz complexes exhibit a ^{3}IL ($\pi \rightarrow \pi^*$) (dppz) emissive state. However, the emission of the dppn complexes possesses substantial ^{3}MLCT ($d\pi(Re) \rightarrow \pi^*$(dppn)) character. These complexes bind to double-stranded calf thymus DNA and synthetic oligonucleotides by intercalation, as revealed by absorption and emission titrations. Upon irradiation, the complexes cleave the DNA plasmid pBR322 efficiently. While the excited complex $[Re(dppz)(CO)_3(py)]^{+*}$ oxidises the DNA molecule directly due to its strong oxidising properties, the dppn complex $[Re(dppn)(CO)_3(py)]^+$ reacts with oxygen upon photoexcitation, resulting in the production of superoxide and hydroxyl radicals that cause DNA strand scissions.

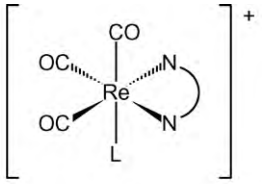

9

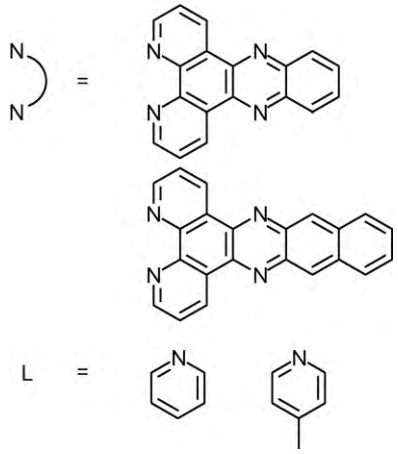

Thomas and co-workers developed DNA probes using dinuclear rhenium(I) dppz complexes such as $[\{Re(dppz)(CO)_3\}_2(py\text{-}CH_2CH_2\text{-}py)]^{2+}$ (**10**) [20]. Unlike their monomeric analogues, these dinuclear complexes are non-emissive in organic solvents and aqueous solutions. Absorption titrations reveal two-stage binding for the two dppz moieties. However, the tether is insufficiently long for both rhenium-dppz units to intercalate into the same duplex. Thus, it is proposed that the complex initially functions as a mono-intercalating probe and the second rhenium-dppz may be free to interact with other DNA duplexes (interstrand binding). In another study, a related heterobimetallic complex $[Ru(tpm)(dppz)(\mu\text{-dpp}[5])(CO)_3Re(dppz)]^{3+}$ (**11**) has been isolated which possesses both DNA-light switch and photocleavage properties [21]. The complex is non-luminescent in aqueous solution but becomes brightly emissive in the presence of DNA. The DNA-binding affinity K_b of the complex is estimated to be $6 \times 10^5\ M^{-1}$. The complex is capable of causing cleavage of DNA upon photoexcitation.

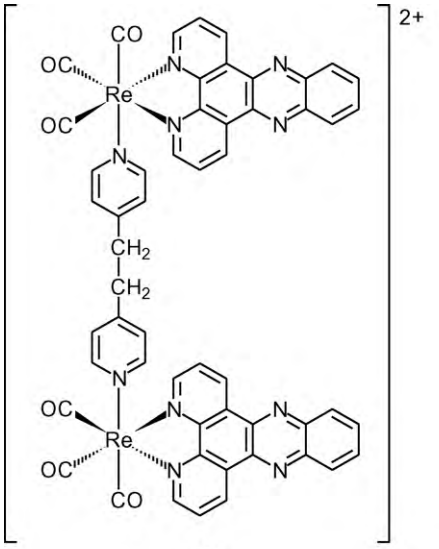

10

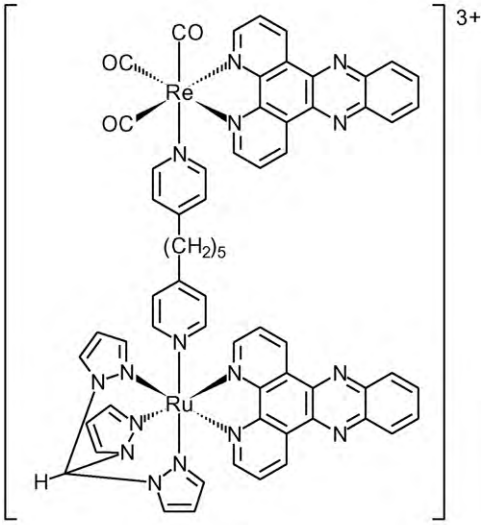

11

2.3. Protein probes

The protein-binding properties of luminescent rhenium(I) polypyridine wires, $[Re(4,7\text{-}Me_2\text{-phen})(CO)_3(\text{imidazole-L})]^+$ (L is a perfluorinated biphenyl bridge containing an imidazole (**12a**) or a fluorine atom (**12b**)) have been studied by Gray and co-workers [22]. Both complexes are luminescent (λ_{em} = 560 nm, Φ_{em} = 0.055 in phosphate buffer) upon excitation. They bind in the active site of the murine iNOSoxy truncation mutants Δ114 and form complexes with it. Binding of complex **12a** shifts the Δ114 haem Soret band from 422 to 426 nm, demonstrating that the terminal imidazole ligates the haem iron. The emission of this complex is strongly quenched in the presence of Δ114, making it a sensitive probe for the enzyme. Emission measurements establish that the dissociation constant for **12a**:Δ114 is 100 ± 80 nM. Upon addition of complex **12b** to Δ114 murine iNOSoxy, the Soret band displays a blue shift and a shoulder appears at ca. 540 nm. This complex binds to Δ114 with a dissociation constant K_d of 5 ± 2 μM, causing partial displacement of water from the haem iron. The findings that both complexes bind in the NOS active site are expected to lead to novel designs of NOS inhibitors.

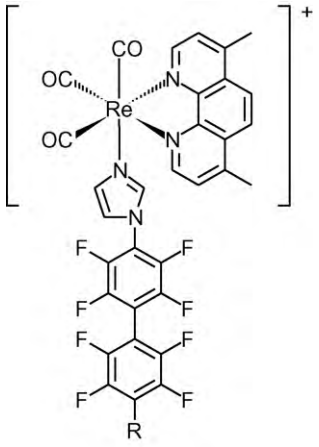

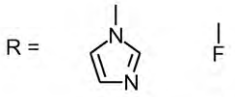

12a **12b**

Lakowicz and co-workers reported the photophysical properties of a rhenium(I) polypyridine complex $[Re(Me_2\text{-}Ph_2\text{-phen})(CO)_3(\text{py-4-COOH})]^+$ (**13**) [23]. The complex shows high emission quantum yield (>0.5) and long emission lifetime (0.3 – 10 μs) in fluid solutions at room temperature. The emission of the complex depends strongly on the polarity of solvents. This complex is activated by NHS and coupled to various biomolecules including HSA, IgG and PE. The conjugates exhibit intense and long-lived emission at ca. 550 nm (τ_o = ca. 4.1–2.8 μs). In a mixture of glycerol and water (6:4, v/v) at −55 °C, the highest values for the initial anisotropy of these conjugates are 0.23, 0.17 and 0.14, respectively. Upon binding to polyclonal anti-HSA, the labelled HSA molecules display a change of the rotational correlation time, resulting in a substantial change in anisotropy. When bound to a protein or lipid, the decay time is ca. 3 μs and the quantum yield is ca. 0.12 in oxygenated aqueous solution at room temperature. These unique photophysical properties and the conjugatability render the complex a potential biomolecular probe. Another rhenium(I) phenanthroline complex equipped with an iodoacetamide moiety $[Re(\text{phen-NHCOCH}_2\text{I})(CO)_3Cl]$ (**14**) has also been conjugated to HSA to give a luminescent conjugate which displays a lifetime of ca. 1 μs [24].

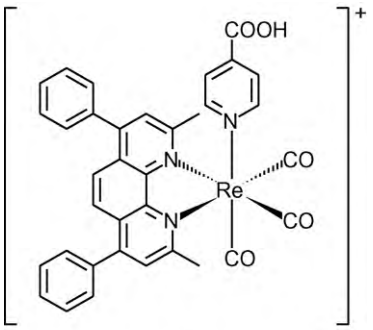

13

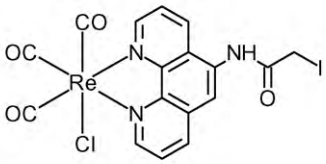

14

Lo et al. reported a series of luminescent rhenium(I) polypyridine isothiocyanate [Re(N^N)(CO)$_3$(py-3-NCS)]$^+$ (**15**) [25] and maleimide [Re(N^N)(CO)$_3$(py-3-mal)]$^+$ (**16**) [26] complexes. These complexes have been used as luminescent biological labels; for example, the phenanthroline complex [Re(phen)(CO)$_3$(py-3-mal)]$^+$ has been conjugated to a cysteine-containing peptide, glutathione (γ-Glu-Cys-Gly) and the proteins BSA and HSA. Upon photoexcitation, the bioconjugates display intense and long-lived yellow ^{3}MLCT (dπ(Re) → π*(phen)) emission in buffer solutions. While the labelled glutathione exhibits a single-exponential decay, both labelled serum albumin conjugates show double-exponential decays with lifetime components of ca. 1.1 and 0.2 μs. The emission quenching of the glutathione conjugate by oxygen is more effective than that of the labelled serum albumins. It is likely that the labels coupled to the proteins are located in a much more hydrophobic environment. Thus, a lower exposure to the solvent surroundings can account for the less efficient oxygen quenching. The long emission lifetimes of these bioconjugates indicate that these rhenium(I) maleimide labels are promising candidates for time-resolved applications.

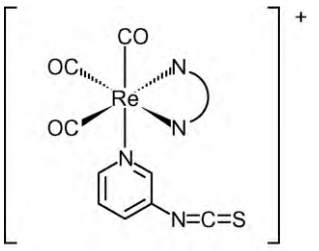

15

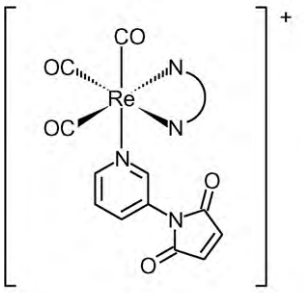

16

The biotin–avidin system has been widely exploited as a powerful tool in bioanalytical applications [27]. Since fluorescent probes play a dominant role in bioanalytical assays, organic fluorophores have been equipped with a biotin moiety [28]. The majority of these compounds suffer from self-quenching upon binding to avidin. The quenching appears to be RET in nature, which is caused by the small Stokes' shifts. Luminescent transition metal complexes have been used as markers or affinity labels in view of their characteristic photophysical properties, in particular, the large Stokes' shifts due to the phosphorescence nature of their emission. The insignificant overlap integrals prevent them from self-quenching when the complexes bind to avidin. The interesting emissive behaviour of rhenium(I) polypyridine complexes promotes the design of new luminescent rhenium(I) polypyridine complexes containing a biotin moiety as new probes for avidin. Lo et al. synthesised a family of luminescent rhenium(I) polypyridine biotin complexes [Re(N^N)(CO)$_3$(py-spacer-biotin)]$^+$ (**17**) [29–32]. Upon irradiation, the complexes display orange to green triplet MLCT (dπ(Re) → π*(N^N)) emission in fluid solutions at 298 K. All the rhenium(I) biotin complexes bind to avidin with the same stoichiometry as unmodified biotin ([Re]:[avidin] = 4:1), which is confirmed by the HABA assay. Remarkably, all the complexes display enhanced emission intensities and extended lifetimes upon binding to avidin. At [Re]:[avidin] = 4:1, the emission intensities of this class of complexes are enhanced by ca. 3.0- to 1.2-fold and the emission lifetimes are extended by ca. 2.4- to 1.3-fold. The first dissociation constants, K_d, range from ca. 5.5×10^{-11} to 3.4×10^{-9} M, which are about 4–6 orders of magnitude larger than that of the native biotin-avidin system (K_d = ca. 10^{-15} M). Using a water-soluble negatively charged polypeptide (poly(D-Glu:D-Lys), 6:4) modified with the non-fluorescent energy-acceptor dye QSY-7 NHS ester as the quencher, the emission enhancement factor for one of the complexes increases from ca. 1.5 to 4.0 upon binding to avidin.

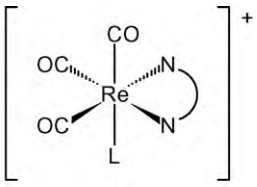

17

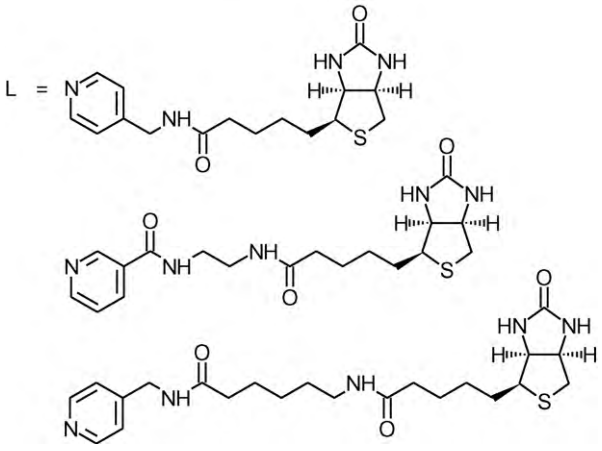

The important physiological properties of indole and its derivatives have been the subject of many biochemical studies. Various approaches have been used to study the substrate-binding properties of indole receptors; for example, radioactive indole derivatives and indole-biotin conjugates have been synthesised and shown to have interesting protein-binding properties. Lo et

al. designed a series of luminescent rhenium(I) polypyridine indole complexes $[Re(N^N)(CO)_3(py\text{-}spacer\text{-}indole)]^+$ (**18**) as probes for indole-binding proteins [33,34]. Upon visible-light irradiation, the complexes exhibit ^{3}MLCT ($d\pi(Re) \rightarrow \pi^*(N^N)$) emission. Interestingly, the rhenium(I) indole complexes show much lower emission quantum yields and shorter emission lifetimes than those of their indole-free counterparts due to self-quenching. Since the excited complexes are very oxidising, ($E^\circ[Re^{+*/0}]$ = ca. +1.25 to +1.49 V vs. SCE), reductive quenching of the excited complexes by the appended indole ($E^\circ[indole^{+/0}] < +1.06$ V vs. SCE) is favoured by a driving force of >0.2–0.4 eV. From this, it can be concluded that the self-quenching of the indole complexes is electron-transfer in nature. The emission intensities of the indole complexes are enhanced in the presence of an indole-binding protein BSA (binding constants are in the order of $10^4\ M^{-1}$). Additionally, the rhenium(I) indole complexes inhibit the indole-binding enzyme tryptophanase. In a related study, luminescent rhenium(I) dpq and dpqa indole complexes $[Re(N^N)(CO)_3(py\text{-}spacer\text{-}indole)]^+$ (N^N = dpq, dpqa) (**19**) are synthesised and characterised [35]. The amide moiety of the dpqa ligand effectively suppresses the emission intensity of the free complexes in aqueous solutions. Thus, the complexes display large BSA-induced emission enhancement factors (ca. 8.0–13.4) (Fig. 1).

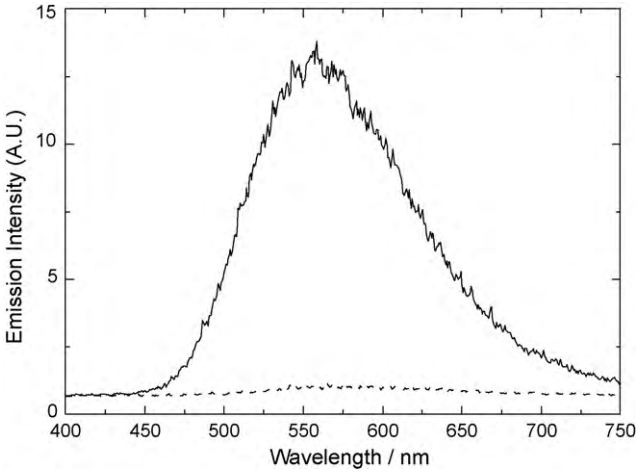

Fig. 1. Time-resolved emission spectra of complex $[Re(dpqa)(CO)_3(py\text{-}spacer\text{-}indole)]^+$ (0.22 mM) in the absence (dashed line) and presence (solid line) of BSA (1 mM) in 50 mM potassium phosphate buffer at pH 7.2/MeOH (95:5, v/v) at 298 K.

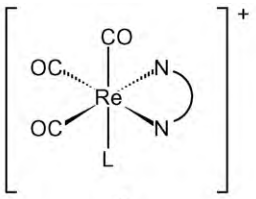

18

L =

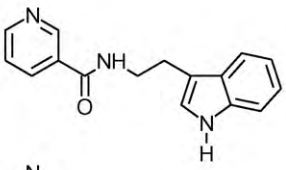

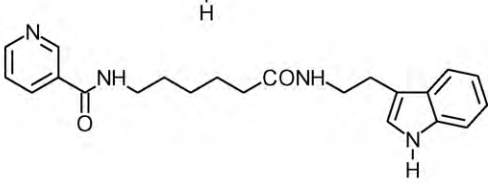

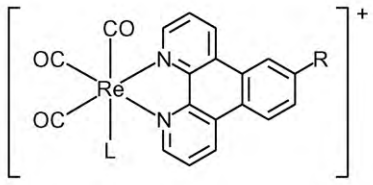

19

R = H

$CONHCH_2CH_2CH_2CH_3$

L =

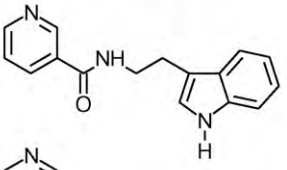

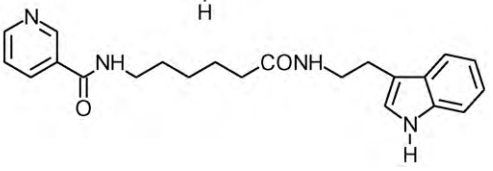

Estradiol is the most potent natural estrogen responsible for the development and maintenance of the secondary sexual characteristics and functions of the reproductive system in females. The physiological effects of estradiol are triggered by its binding to

estrogen receptors. Owing to the important roles of both estradiol and its receptor on female physiology, the design of new biological probes for estradiol-binding proteins has been focused. Lo et al. reported a class of rhenium(I) polypyridine estradiol complexes $[Re(N^N)(CO)_3(py\text{-}spacer\text{-}estradiol)]^+$ (**20**) that exhibit intense and long-lived ^{3}MLCT ($d\pi(Re) \rightarrow \pi^*(N^N)$) emission upon irradiation [36]. In the presence of ERα, the emission intensities of the py-C6-est complexes are enhanced (ca. 5.1- to 6.1-fold) and the emission maxima are blue-shifted, suggestive of increased hydrophobicity and rigidity of the local environments of the complexes. The binding constants of these complexes to ERα are estimated to be in the order of 10^7 M^{-1}, which are two orders of magnitude smaller than that of unmodified estradiol ($K_a = 5 \times 10^9$ M^{-1}). The lower binding affinity is a result of the bulkiness of rhenium(I) polypyridine moieties.

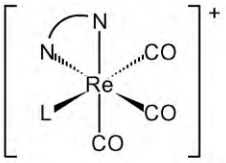

20

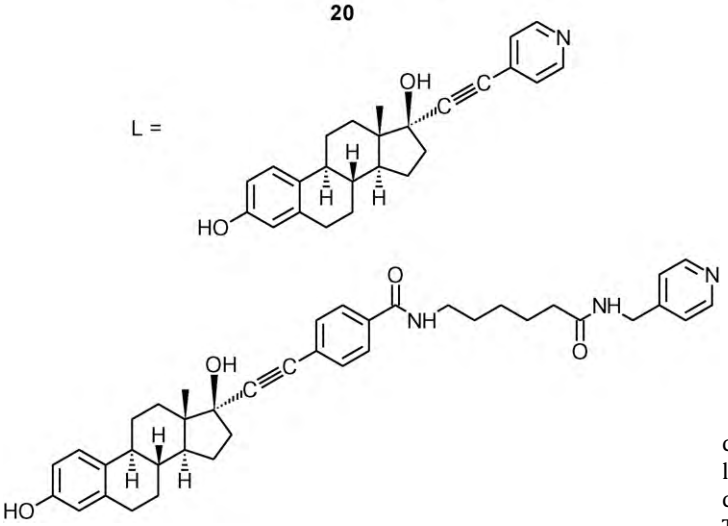

2.4. Cellular probes

Coogan and co-workers designed lipophilic and hydrophilic rhenium(I) polypyridine complexes $[Re(N^N)(CO)_3(py\text{-}3\text{-}R)]^+$ (N^N = bpy, phen{C_6H_4-SO_3^-}$_2$; R = CH_2OH, H) (**21**) [37]. The bpy complexes contain aliphatic chains of different lengths, which render the complexes more lipophilic. All the complexes show typical ^{3}MLCT emission at ca. 555 nm in CH_3CN and at ca. 565 nm in water. In order to test the viability of these complexes as fluorophores in cell microscopy, their ability to act as microscopy stains is tested in *Spironucleus vortens*, a parasitic flagellate which is found in many species of fish [38]. Upon incubation for 2 h, the complexes are uptaken by the cells as revealed in the confocal images (λ_{ex} = 405 nm). The highly lipophilic bpy complexes are toxic at high concentrations, apparently disrupting the membranes and leading to cell lysis. The hydrophilic complex $[Re(phen\{C_6H_4\text{-}SO_3\}_2)(CO)_3(py\text{-}CH_2OH)]^-$ is less cytotoxic and it appears that localisation in digestive vacuoles occurs by phagocytosis. Also, a related rhenium(I) complex containing a chloromethylpyridine ligand $[Re(bpy)(CO)_3(py\text{-}3\text{-}CH_2Cl)]^+$ (**22**) has been developed as a sulfhydryl-specific label. Incubation of the complex with MCF-7 cells results in efficient cellular uptake, as revealed by confocal microscopy. The microscopy images suggest localisation of the complexes in mitochondria, which is in accordance with the cationic, lipophilic and thiol-reactive nature of the complex.

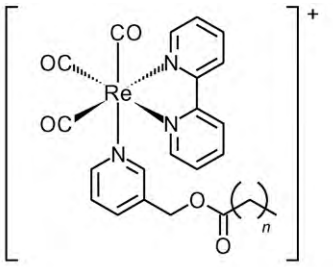

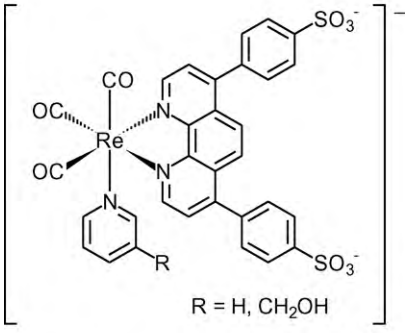

21

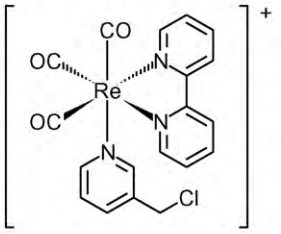

22

Zubieta and co-workers reported a luminescent rhenium(I) complex (**23**) containing a tridentate ligand (quinoline-CH_2)$_2$-NR linked to an *N*-α-Fmoc-L-lysine unit [39]. Upon photoexcitation, the complex shows two distant emission maxima at 425 and 580 nm. The quantum yield of the complex ranges from 0.003 in aerated $CHCl_3$ to 0.015 in degassed ethylene glycol. The lifetime varies from 4.31 to 9.76 μs depending on the solvents and the amount of oxygen present. The complex can be incorporated into peptides as if it were a natural amino acid. Using a conventional automated synthesiser, it is integrated within fMLF, a targeting sequence which is used to guide radionuclides to the formyl peptide receptor (FPR). The affinity of the complex to the receptor is determined using flow cytometry ($K_d = 27 \pm 13$ nM). The cellular uptake of rhenium fMLF bioconjugate is studied using fluorescence microscopy. At low temperatures, the bioconjugate binds to the periphery of the leukocytes but it is internalised into the cytoplasm of the cells when the sample is allowed to warm to room temperature. Colocalisation of the bioconjugate and a well-established fluorescent FPR probe confirms that they target the same cell populations.

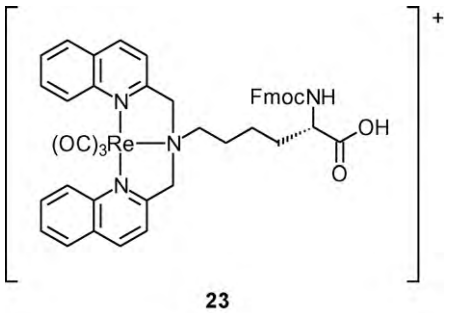

23

Lo and co-workers reported the first class of luminescent biotinylation reagents derived from rhenium(I) polypyridine complexes $[Re(N^N)(CO)_3(py\text{-}biotin\text{-}NCS)]^+$ (**24a**) [40]. To investigate the amine-specific reactivity of the isothiocyanate complexes, they have been reacted with a model substrate ethylamine, resulting in the formation of the thiourea complexes $[Re(N^N)(CO)_3(py\text{-}biotin\text{-}TU\text{-}Et)]^+$ (**24b**). The avidin-binding properties of the thiourea complexes have been examined by the HABA assay and emission titrations (I/I_o = ca. 1.4–1.5). Additionally, BSA has been biotinylated with the isothiocyanate complexes, affording protein conjugates that display intense and long-lived orange-yellow to greenish-yellow emission upon irradiation. The cytotoxicity of the thiourea complexes towards the HeLa cells has been examined by the MTT assay. The IC_{50} values are between ca. 17.5 and 28.5 μM, which are comparable to that of cisplatin (26.7 μM) under the same experimental conditions. The cellular uptake of one of the thiourea complexes $[Re(Ph_2\text{-}phen)(CO_3)(py\text{-}biotin\text{-}TU\text{-}Et)]^+$ has been investigated by fluorescence microscopy, and the results show that the complex is localised in the perinuclear region (Fig. 2).

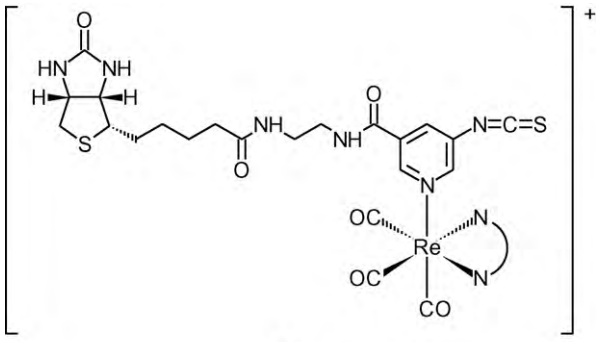

24a

Lo and co-workers reported two luminescent rhenium(I) polypyridine bis-biotin complexes with different spacer-arms $[Re(N^N)(CO)_3(py)]^+$ (**25**) (N^N = bpy-CONH-C2-NH-biotin2, bpy-CONH-C2-NHCO-C6-NH-biotin2) [41]. The biotin pendants are attached to the diimine ligand of the complexes, which is involved in the ^{3}MLCT emissive state. Upon irradiation, the complexes display orange to red ^{3}MLCT emission in fluid solutions. HABA assay reveals that both bis-biotin complexes show an equivalent point at [Re]:[avidin] ≈ 2.5. The value is <4, suggesting that both biotins are functional but the binding is not sufficiently strong and/or both biotin moieties of the complex are not functional simultaneously, possibly due to steric hindrance. The complexes exhibit

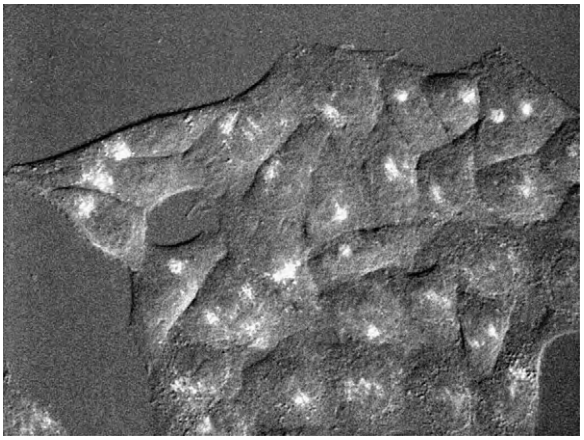

Fig. 2. Fluorescence and brightfield overlaid microscopy image of HeLa cells incubated with complex $[Re(Ph_2\text{-}phen)(CO)_3(py\text{-}biotin\text{-}TU\text{-}Et)]^+$ (10 μM) at 37 °C for 24 h.

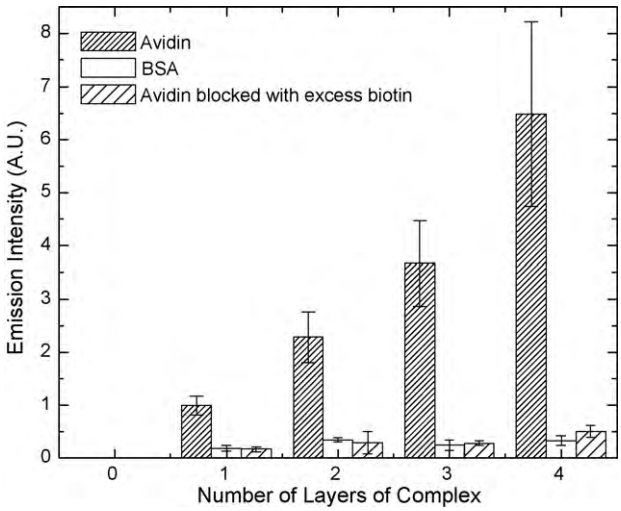

Fig. 3. Averaged emission intensities of avidin-modified microspheres ($N = 6$) upon incubation of zero to four layers of $[Re(bpy\text{-}CONH\text{-}C2\text{-}NHCO\text{-}C6\text{-}NH\text{-}biotin2)(CO)_3(py)]^+$. The results of the control experiments (BSA is used instead of avidin or when the avidin is presaturated with biotin from the outset) are included.

emission enhancement and lifetime extension in the presence of avidin. The potential use of the complexes as signal amplifiers for heterogeneous recognition assays is demonstrated using avidin-coated microspheres and $[Re(bpy\text{-}CONH\text{-}C2\text{-}NHCO\text{-}C6\text{-}NH\text{-}biotin2)(CO)_3(py)]^+$. After immobilisation of four layers of the complex, the average emission intensity of the microspheres is about 6.5 times higher than that of that immobilised with only one layer, indicating that the increased emission intensity results from the avidin-crosslinking properties of the complex (Fig. 3). The MTT assay shows that these complexes are basically noncytotoxic (IC_{50} values estimated to be >250 μM). The possibility of using these complexes as imaging reagents for live cells has been investigated using laser-scanning confocal microscopy. HeLa cells treated with all the complexes showed localisation in the perinuclear region with much weaker or no emission from the nuclei, indicative of negligible nuclear uptake or net exclusion of the complexes from the nucleus.

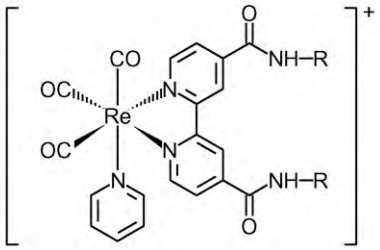

25

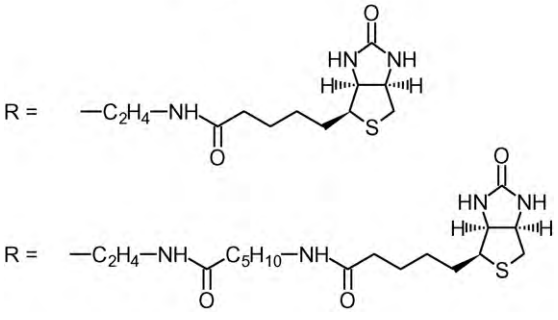

In view of sensing capabilities and efficient cellular uptake of luminescent rhenium(I) polypyridine complexes, functionalisation of this type of complexes for cellular sensing applications is a

very interesting area of research. Luminescent rhenium(I) polypyridine complexes $[Re(N^N)(CO)_3(py\text{-}TU\text{-}DPAT)]^+$ (**26a**) containing a tyramine-derived 2,2′-dipicolylamine unit and their DPAT-free counterparts $[Re(N^N)(CO)_3(py\text{-}TU\text{-}Et)]^+$ (**26b**) have been designed by Lo and co-workers [42]. The DPAT complexes show lower emission quantum yields and shorter lifetimes compared to their DPAT-free counterparts, suggestive of a self-quenching process in which the emission of the rhenium(I) polypyridine unit is quenched by the DPAT moiety. Additionally, the incorporation of a DPAT moiety into the rhenium(I) polypyridine complexes results in pH-dependent emission of these complexes. An example is shown in Fig. 4. In general, at pH <3, the DPAT complexes show relatively intense emission. Upon increasing the pH, the emission intensity decreases substantially, and at pH >11, the emission is almost completely quenched. This supports the hypothesis that the amine of the DPAT quenches the emission of the complexes. Upon addition of zinc(II) or cadmium(II) ions, the DPAT complexes reveal emission enhancement (I/I_o = ca. 1.8–3.9) and lifetime extension (τ/τ_o = ca. 1.4–1.6). Apparently, the coordination of the amine of the DPAT unit to the metal ions substantially suppresses the self-quenching of the complexes, leading to the observed emission enhancement and lifetime extension. The dissociation constants of the adducts formed from the DPAT complexes and the ions, are on the order of 10^{-5} to 10^{-6} M. The cellular uptake efficiency of all the complexes by HeLa cells is determined. ICP-MS measurements reveal that the cellular uptake of the DPAT complexes is higher than the DPAT-free complexes. The MTT assay shows that all the complexes are more cytotoxic than cisplatin. Treatment of HeLa cells with the complexes leads to almost full cytoplasmic staining but negligible localisation in the nucleoplasm and nucleoli. The intracellular ion-binding properties of $[Re(Ph_2\text{-}phen)(CO)_3(py\text{-}TU\text{-}DPAT)]^+$ have been studied. The emission intensity of an average cell is increased by ca. 2.2- and 1.8-fold after treatment with zinc(II) and cadmium(II) ions, respectively (Fig. 5).

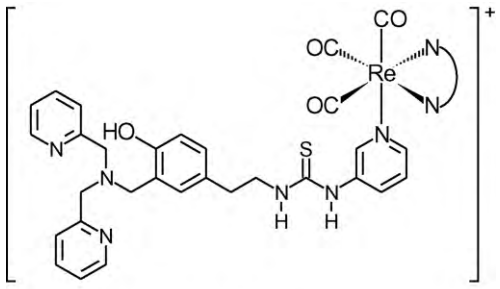

26a

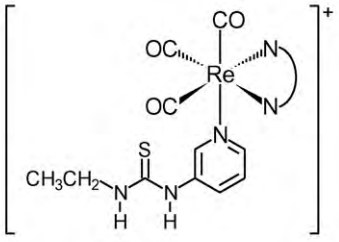

26b

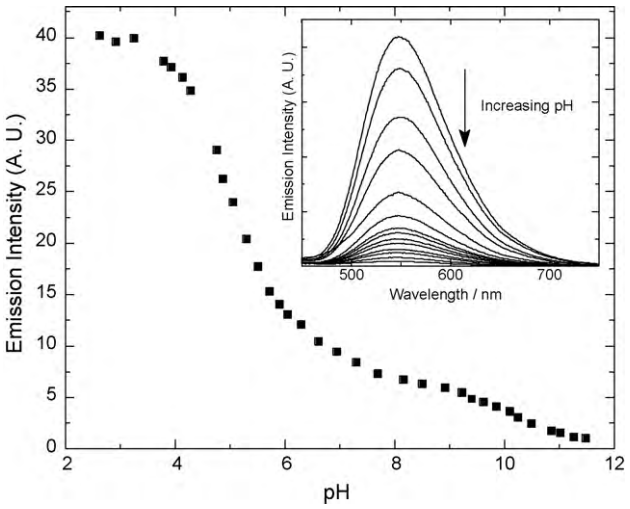

Fig. 4. pH titration curve for complex $[Re(phen)(CO)_3(py\text{-}TU\text{-}DPAT)]^+$ in aerated 100 mM KCl(aq)/MeOH (7:3, v/v) at 298 K. The inset shows the emission spectral traces upon increasing pH.

3. Iridium(III) complexes

3.1. Ion and small molecule probes

Huang and co-workers reported the synthesis and properties of a series of luminescent iridium(III) imidazo[4,5-*f*][1,10]phenanthroline complexes such as (**27**) [43]. The influences of proton and anions on the photophysical and electrochemical properties have been studied. Upon addition of H^+, the emission wavelength is significantly red-shifted and the emission colour changes from yellow to red. Addition of F^-, $CH_3COO^-$and $H_2PO_4^-$ also causes significant variations in the UV–vis absorption and emission spectra. The colour of the solutions changes from greenish-yellow to brown and the emission is quenched completely.

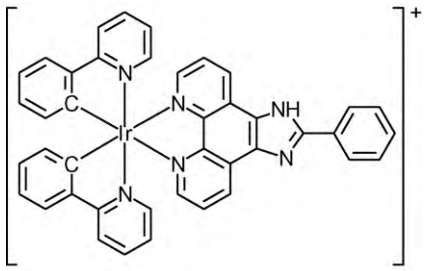

27

The same research group designed an iridium(III) complex $[Ir(pba)_2(acac)]$ (**28**) as a sensor for homocysteine [44]. Upon addition of homocysteine, the complex shows a colour change from orange to yellow while the emission colour changes from deep red to green. These findings are attributed to the formation of a thiazinane group by the reaction of the aldehyde group in the ligand pba with homocysteine. This sensing property is unique towards homocysteine over other amino acids and thiol-related peptides.

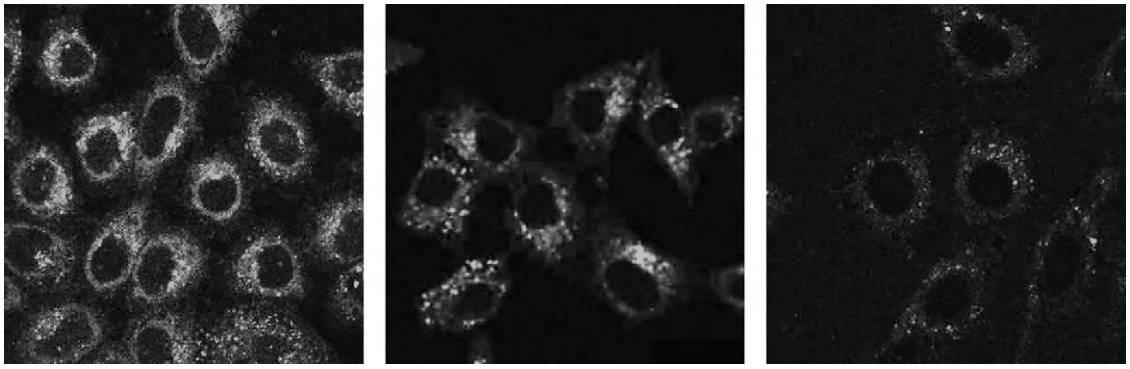

Fig. 5. Laser-scanning confocal microscopy images of HeLa cells incubated with $[Re(Ph_2\text{-phen})(CO)_3(py\text{-TU-DPAT})]^+$ (5 μM) at 37 °C for 1 h followed by incubation of zinc(II) chloride/MPO (25 μM) (left), cadmium(II) chloride/MPO (25 μM) (middle) and MPO (25 μM) only (right) for 5 min.

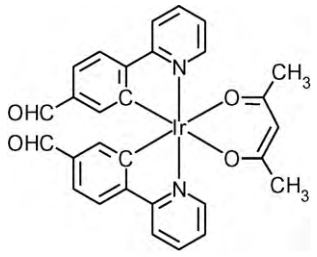

28

Li and co-workers reported a phosphorescent iridium(III) complex $[Ir(Bpq)_2(bpy)]^+$ (**29**) containing bis-mesitylboryl groups [45]. Both the ligand Bpq and the complex are used as highly selective chemosensors for fluoride. The emission band of the free ligand Bpq exhibits a red shift upon addition of fluoride ion. This is account for by the switch of the excited state from ^{3}IL ($\pi \rightarrow \pi^*$) to CT transition. Addition of fluoride ion induces a colour change of a solution of complex **29** from yellow to orange-red and causes substantial emission quenching. TDDFT calculations show that the complexation of the mesitylboryl groups with fluoride ion significantly changes the excited-state properties of the complex.

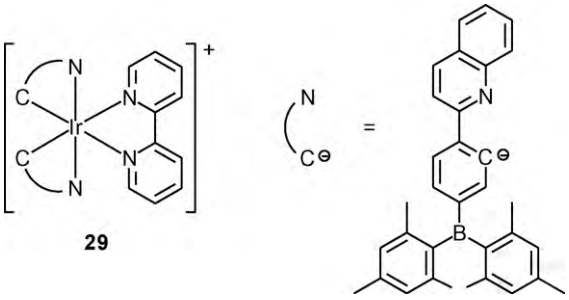

29

Goodall and Williams reported iridium(III) bis-terpyridine complexes (**30**) with a *m*- or *p*-*N*-methylpyridinium substituent at the terpyridine 4′-position [46]. Both complexes display long-lived luminescence in aqueous solution and that of the *meta*-isomer is quenched by chloride ion at physiologically relevant concentrations. In contrast to typical fluorescent sensors, the emission lifetimes are on the microsecond timescale. Both the intensity and the lifetime are perturbed by chloride ion with good selectivity over many other anions, rendering the complex a potential sensory system for chloride ion. Additionally, the same group prepared a series of homoleptic iridium(III) bis-terpyridine complexes appended with pyridine groups at the 4′-positions of one or both of the terpyridine ligands and their heteroleptic analogues with ttpy as an ancillary ligand [47]. All the complexes are luminescent in air-equilibrated aqueous solution at room temperature. The homoleptic complexes display structured emission which resembles that of the unsubstituted complex $[Ir(tpy)_2]^{3+}$ (τ_o = ca. 1 μs). The heteroleptic analogues give broader and red-shifted emission spectra, similar to that of $[Ir(ttpy)_2]^{3+}$, indicative of a lower energy ttpy-based emissive state. A further red shift for the complexes incorporated with an additional phenyl ring reveals that the emissive state involves the more conjugated phenylpyridyl-appended ligand in these cases. Both the emission intensity and lifetimes of the heteroleptic complexes (except the *meta*-substituted system) are reduced upon protonation of the pendent pyridine group. Interestingly, the behaviour of the *meta*-phenylpyridyl-substituted system is different as it shows an increase in emission intensity and a blue shift in the spectrum upon protonation.

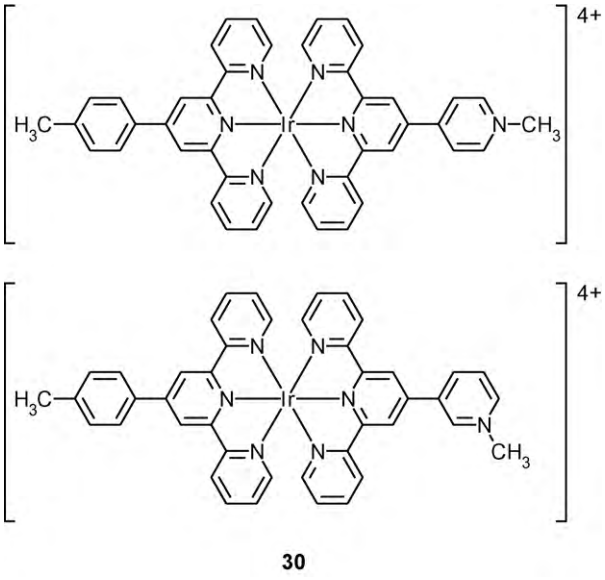

30

Chi and co-workers reported an iridium(III) complex (**31**) that contains an 1-aza-15-crown-5-ether-substituted pyridyl pyrazolate as a metal cation probe [48]. The absorption bands at 315 and 375 nm are assigned to ^{1}IL ($\pi \rightarrow \pi^*$) transitions incorporating pyrazolates → pyridyl types of charge-transfer. The emission band at 560 nm reveals a drastic oxygen quenching effect, the intensity of which decreases from 0.22 in degassed CH_3CN, to ca. 1.0×10^{-3} upon aeration. Addition of metal ions, including Ca^{2+}, Mg^{2+}, Ba^{2+} and Na^+, leads to a hypsochromic shift of the absorption profile, in which the appearance of an isosbestic point at ca. 295 nm verifies a two-species equilibrium. Upon excitation at the isosbestic point, the phosphorescence is gradually blue-shifted, accompanied by an increase of the emission intensity. Additionally, the success in the recognition of Ca^{2+}(aq) in the TLC plate demonstrates its suitability for the future development of a practical device, such as a metal ion sensor anchored on cellular membranes.

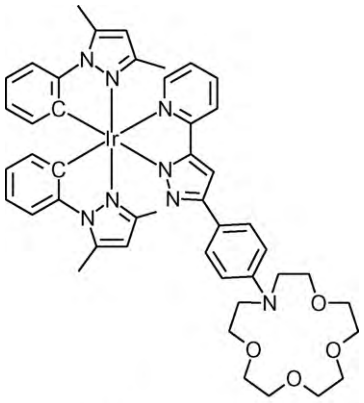

31

Lo et al. isolated a family of luminescent cyclometallated iridium(III) polypyridine thiourea complexes $[Ir(N^{\wedge}C)_2(N^{\wedge}N)]^+$ (HN^C = Hppy, Hbzq, Hpq; N^N = phen-TU-Et, phen-TU-Ph, phen-TU-MeA) (**32**) [49]. Upon irradiation, the iridium(III) thiourea complexes display intense and long-lived luminescence under ambient conditions and in low-temperature alcohol glass. The emission is assigned to a ^{3}MLCT ($d\pi(Ir) \rightarrow \pi^*(N^{\wedge}C)$) excited state. However, the pq complexes show very long emission lifetimes and structured emission bands, which indicate that the excited state has substantial ^{3}IL ($\pi \rightarrow \pi^*$(pq)) character. The emission intensities of all the complexes are reduced upon addition of acetate, fluoride and dihydrogen phosphate ions; an example is illustrated in Fig. 6. The binding stoichiometry is determined to be 1:1 in all cases and the log K_b values range from 3.12 to 4.35. The affinity of the thiourea complexes towards acetate ion is higher than that towards fluoride and dihydrogen phosphate ions, which is attributed to a combined effect of the basicity and molecular geometry of the anions.

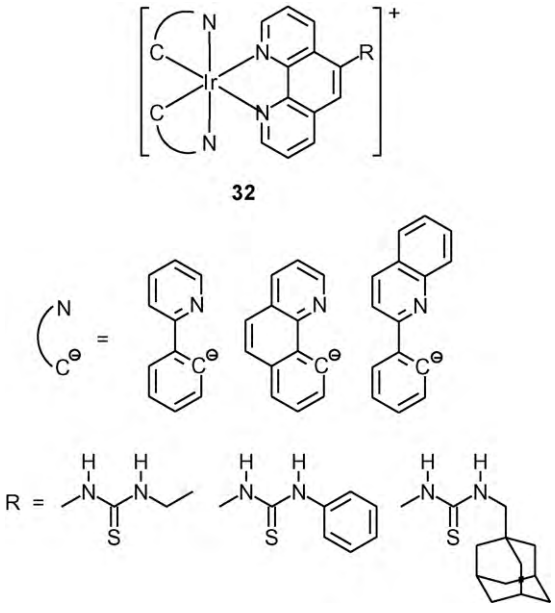

32

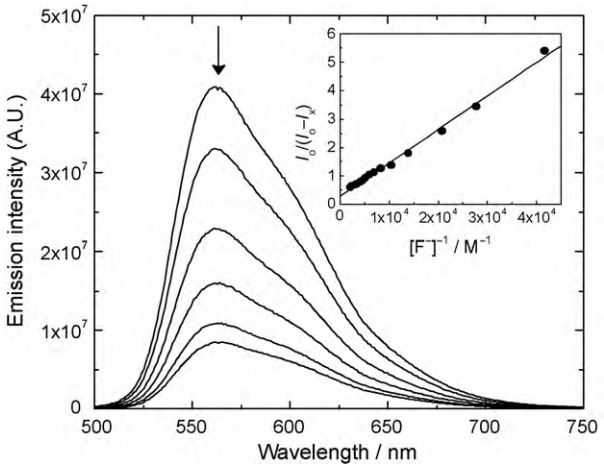

Fig. 6. Emission spectral traces of complex $[Ir(pq)_2(phen\text{-}TU\text{-}MeA)]^+$ (120 μM) in CH_3CN (0.1 M TBAP) upon addition of F^- at 298 K. The concentrations of F^- were 0, 24, 48, 72, 96 and 120 μM, respectively. Inset: a plot of $I_o/(I_o - I_x)$ vs. $[F^-]^{-1}$ and the theoretical fit on the basis of a 1:1 binding stoichiometry.

3.2. DNA probes

Lo et al. designed a series of cyclometallated iridium(III) dipyridoquinoxaline and dipyridophenazine complexes $[Ir(ppy)_2(N^{\wedge}N)]^+$ (N^N = dpq, dpqa, dppz, dppn) (**33**) as luminescent intercalators for DNA [50]. Upon excitation, these complexes display intense and long-lived green to orange ^{3}MLCT or ^{3}IL luminescence in aprotic organic solvents at room temperature and in low-temperature glass. In aqueous solution, these complexes are weakly or non-emissive due to the possible hydrogen-bonding interactions between the phenazine nitrogen atoms (and the amide moiety of the dpqa complexes) and H_2O molecules. The binding of these complexes to double-stranded calf thymus DNA and synthetic double-stranded oligonucleotides poly(dA)·poly(dT) and poly(dG)·poly(dC) is investigated by spectroscopic titrations. Upon addition of double-stranded calf thymus DNA or synthetic double-stranded oligonucleotides, the absorption bands of the dppz and dppn complexes exhibit hypochromism and bathochromic shifts, suggesting that the complexes bind to the double-stranded DNA or oligonucleotides molecules, probably through a non-covalent intercalative binding mode. The binding affinities of the dppz and dppn complexes to calf thymus DNA ($K = 2.0 \times 10^4$ and 7.8×10^4 M^{-1}, respectively) are comparable to those to poly(dA)·poly(dT) ($K = 2.3 \times 10^4$ and 7.6×10^4 M^{-1}, respectively) but higher than those to poly(dG)·poly(dC) ($K = 1.0 \times 10^4$ and 5.0×10^4 M^{-1}, respectively). These four complexes display emission enhancement in the presence of double-stranded calf thymus DNA. The emission intensity of the dpq complex at ca. 591 nm is enhanced by ca. 33-fold. New emission bands are observed at around 602 and 606 nm for the proton induced non-emissive dpqa and dppz complexes, respectively. These changes are ascribed to the intercalation of the complexes into the base pairs of the double-stranded DNA molecules, resulting in increased hydrophobicity and rigidity of the local surroundings of the complexes and the protection of the N^N ligands from interacting with the H_2O molecules. Emission titrations with synthetic double-stranded oligonucleotides show similar results.

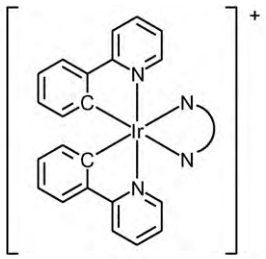

33

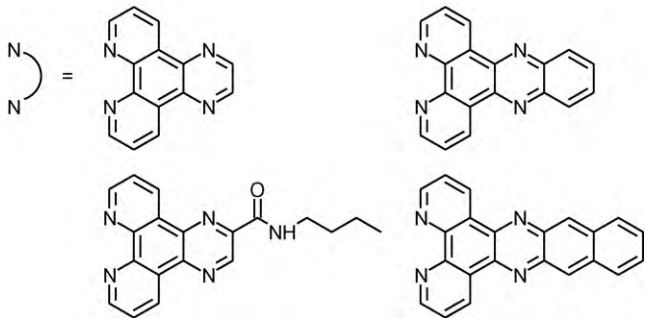

Barton and co-workers synthesised a tris(heteroleptic) iridium(III) phenanthrenequinone diimine complex $[Ir(bpy)(phen)(phi)]^{3+}$ (**34**) through the stepwise introduction of three different bidentate ligands [51]. The Λ- and Δ-enantiomers are resolved and characterised by CD spectroscopy. The complex binds strongly to DNA by intercalation. Electrochemical studies show that the complex undergoes a reversible one-electron phi-based reduction at $E^{\circ} = -0.025$ V (vs. Ag/AgCl) in 0.1 M TBAH/DMF. The EPR spectrum of the electrochemically generated species $[Ir(bpy)(phen)(phi)]^{2+}$ is consistent with a phi-based radical. The electrochemistry of complex **34** is also probed at a DNA-modified electrode, where a binding affinity of $K = 1.1 \times 10^6\ M^{-1}$ is measured. In contrast to the free complex in solution, the DNA-bound complex undergoes a concerted two-electron reduction to form a diradical species. On the basis of the results from UV–vis and EPR spectroscopy, disproportionation of electrochemically generated $[Ir(bpy)(phen)(phi)]^{2+}$ occurs upon DNA binding. The same group reported cyclometallated iridium(III) dppz complexes [52]. Luminescence and EPR measurements of the iridium(III) complex with an unmodified dppz bound to DNA show the formation of a guanine radical upon irradiation, resulting from an oxidative photoinduced electron-transfer process. Cyclopropylamine-substituted nucleosides have been utilised as ultrafast kinetic traps to report transient charge occupancy in oligonucleotides when DNA is irradiated in the presence of non-covalently bound complexes. These results reveal that the excited state of the derivatised iridium(III) complexes can trigger the oxidation of guanine and the reduction of cytosine.

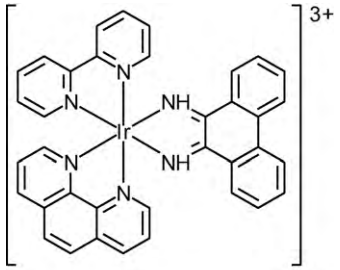

34

3.3. Protein probes

Wong and co-workers synthesised a new luminescent switch-on probe $[Ir(ppy)_2(solvent)_2]^+$ (**35**) for histidine/histidine-rich proteins and demonstrated its utility in protein staining [53]. The complex $[Ir(ppy)_2(CH_3CN)_2]^+$ is weakly emissive in PBS. In the presence of histidine (His), it exhibits an intense emission band at 505 nm, the intensity of which is increased by up to 180-fold and reaches saturation level at [His]:[Ir] ≥ 4. Similar emission enhancement is also observed in competition experiments involving His and 10 equivalents of another natural amino acid, indicating the His-selectivity of this complex. The ESI-MS analysis suggests that this iridium(III) solvent complex may specifically recognise His through covalent attachment to the imidazole moiety of His instead of the carboxylate group of other natural amino acids. In the presence of BSA, which has a relatively high number of His residues, this complex displays intense emission at 505 nm, the intensity of which is increased by up to 800-fold and reaches saturation level at [BSA]:[Ir] ≥ 100. In addition, the staining of a series of proteins in SDS-PAGE with the complex is examined and the lowest quantity of the protein detected after staining is as low as 1.5 ng.

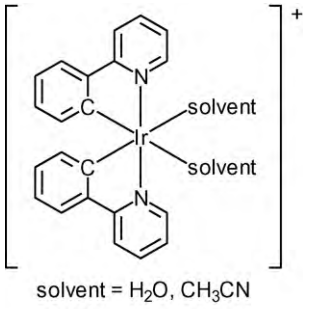

solvent = H_2O, CH_3CN

35

The development of non-covalent probes for proteins commonly relies on the substrate-binding sites of protein. A series of luminescent cyclometallated iridium(III) bipyridine complexes $[Ir(N^{\wedge}C)_2(N^{\wedge}N)]^+$ (HN^C = Hppy, Hppz, Hbzq, Hpq, Hbsb; N^N = bpy-spacer-estradiol (**36**) [54], bpy-spacer-indole (**37**) [55]), containing an estradiol or an indole moiety, is designed by Lo and co-workers to probe estrogen receptors and indole-binding proteins, respectively. Upon photoexcitation, all the complexes exhibit intense and long-lived greenish-yellow to orange emission in fluid solutions under ambient conditions and in low-temperature glass. The emission is assigned to a ^{3}MLCT ($d\pi(Ir) \rightarrow \pi^*(N^{\wedge}N)$) or ^{3}IL ($\pi \rightarrow \pi^*(N^{\wedge}C$ or $N^{\wedge}N)$) excited state. The iridium(III) estradiol conjugates show specific binding to ERα (binding constants, $K_a = 1.0 \times 10^7$ to $2.1 \times 10^7\ M^{-1}$) and display emission enhancement (1.3- to 4.8-fold) and lifetime extension in the presence of this receptor. When ferricyanide is used as a quencher, the ERα-induced emission enhancement is much more significant (7.7- to 48.7-fold) (Fig. 7). This is ascribed to the immobilisation of the complexes by the protein matrix, which renders the quenching by ferricyanide ion more difficult. The interactions of the iridium(III) indole complexes with an indole-binding protein, BSA, are studied by emission titrations. Emission enhancement (2.2- to 12.6-fold) and lifetime elongation are both observed upon addition of BSA. The K_a values are on the order of $10^4\ M^{-1}$.

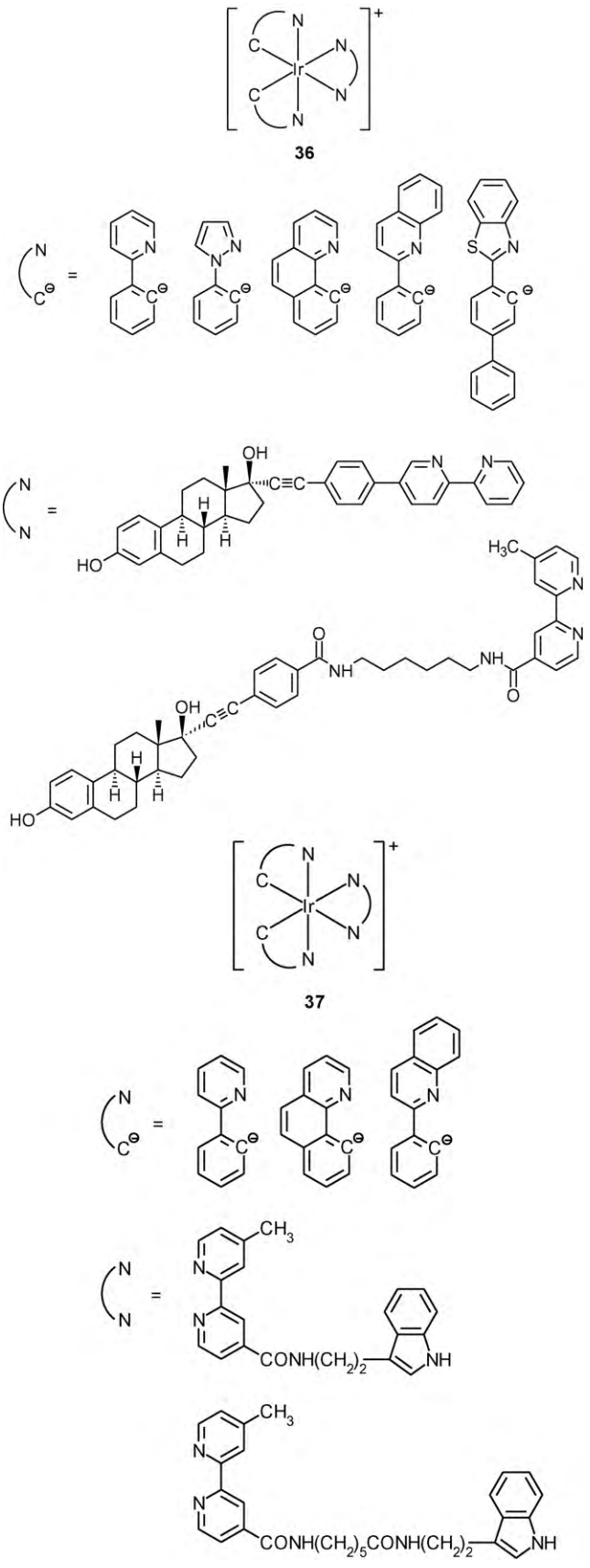

36

37

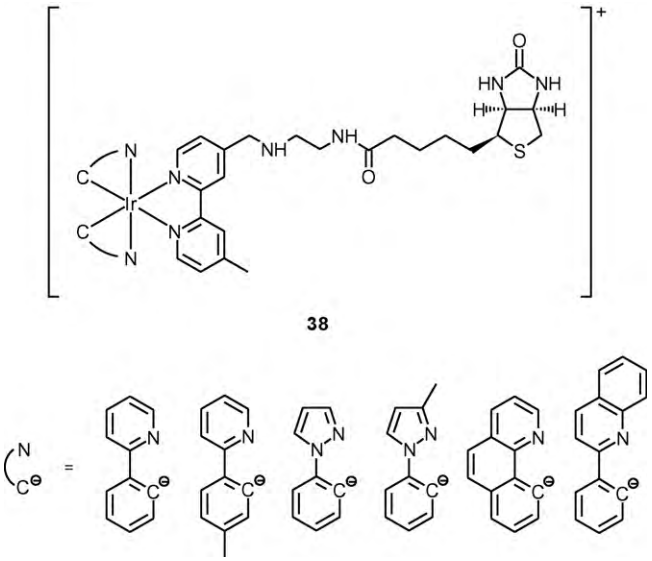

38

A series of luminescent cyclometallated iridium(III) polypyridine complexes equipped with a biotin moiety $[Ir(N^{\wedge}C)_2(bpy\text{-}en\text{-}biotin)]^+$ (HN^C = Hppy, Hmppy, Hppz, Hmppz, Hbzq, Hpq) (**38**) has been synthesised and characterised [56]. Upon excitation, all the complexes show intense and long-lived orange to greenish-yellow luminescence in fluid solutions under ambient conditions and in low-temperature glass. Emission titrations show that all the complexes display enhanced emission intensities (ca. 1.5- to 3.3-fold) and extended emission lifetimes (ca. 1.5- to 3.3-fold) upon binding to avidin, and the dissociation constant K_d are between 2.0×10^{-10} and 2.0×10^{-8} M. Another series of luminescent cyclometallated iridium(III) arylbenzothiazole biotin complexes $[Ir(N^{\wedge}C)_2(bpy\text{-}CONH\text{-}C6\text{-}NH\text{-}biotin)]^+$ (HN^C = Hbt, Hbsb, Hbtth, Hbsn) (**39**) has been designed [57]. These are typical ^{3}IL ($\pi \rightarrow \pi^*$) (N^C) emitters, which show intense green to red emission under ambient conditions. In the presence of avidin, all these complexes display enhanced emission intensities and extended emission lifetimes. Interestingly, the more hydrophobic bsb and bsn complexes reveal more significant emission enhancement (ca. 8.1- and 5.8-fold, respectively). To maximise the difference in emission

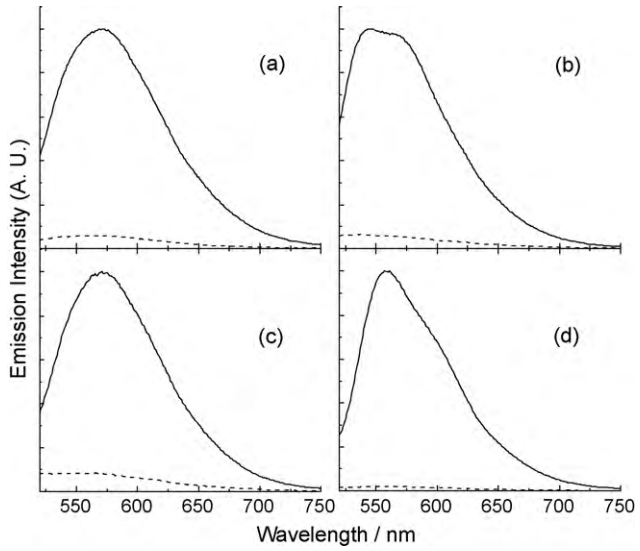

Fig. 7. Emission spectra of $[Ir(N^{\wedge}C)(bpy\text{-}spacer\text{-}estradiol)]^+$ (N^C = ppy (a), ppz (b), bzq (c) and pq (d)) in the absence (dashed line) and presence (solid line) of ERα (375 nM) in potassium phosphate buffer (50 mM, pH 7.4)/methanol (9:1) at 298 K containing 100 μM $[Fe(CN)_6]^{3-}$.

intensities between the free and avidin-bound forms of the complexes, two new luminescent cyclometallated iridium(III) biotin complexes $[Ir(ppy)_2(N^\wedge N)]^+$ (N^N = dpq-CONH-C2-NH-biotin and dppz-CONH-C2-NH-biotin) (**40**) containing the dipyridoquinoxaline and dipyridophenazine ligands are designed [50]. Upon excitation, these complexes display long-lived green to orange luminescence in nonpolar organic solvents, but both are non-emissive in aqueous buffer. However, addition of avidin leads to the appearance of a new emission band with peak maximum at 490 nm and a shoulder at around 520 nm. The new emission band is ascribed to a ^{3}IL ($\pi \rightarrow \pi^*$) (N^N) excited state. At a ratio of [Ir]:[avidin] = 4, the emission intensities of the iridium(III) dpq and dppz biotin complexes at 490 nm are increased by ca. 31- and 8-fold, respectively. The K_d values are determined to be 2.0×10^{-7} and 8.2×10^{-7} M, respectively.

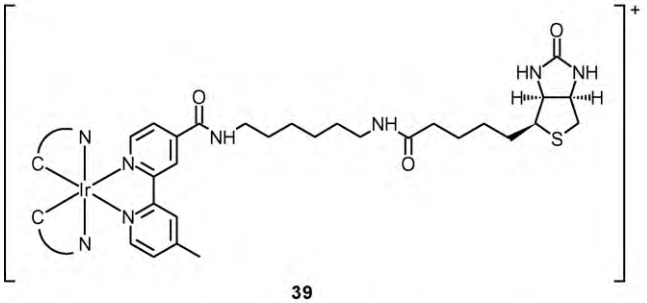

39

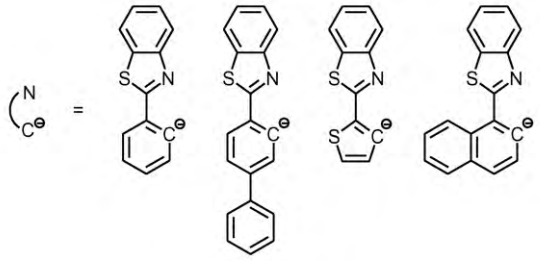

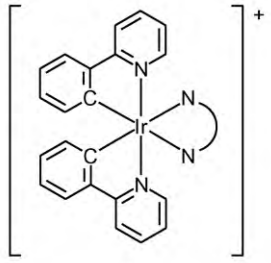

40

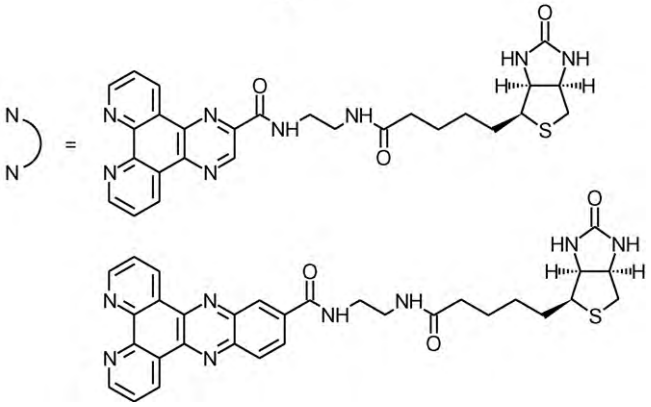

To make use of the four biotin-binding sites of avidin and to amplify the detecting signal of the system, multi-biotin reagents are designed to crosslink labelled avidin. Wilbur et al. synthesised a number of biotin dimers and trimers [58,59]. The ability of these compounds in polymerisation and crosslinking of r-SAv is investigated by size-exclusion chromatography and heterogeneous assays. Biotin trimers show higher potential to crosslink r-SAv than biotin dimers. Lo and Lau reported a series of luminescent cyclometallated iridium(III) polypyridine bis-biotin complexes $[Ir(N^\wedge C)_2(N^\wedge N)]^+$ (HN^C = Hppy-4-CH_2-NH-C2-NH-biotin, Hppy-4-CH_2-NH-C6-NH-biotin; N^N = Me_4-phen, Ph_2-phen) (**41**) [60]. Each complex contains two biotin units with two different spacer-arms between the iridium(III) centre and the biotin moiety. All the complexes display intense and long-lived ^{3}MLCT ($d\pi(Ir) \rightarrow \pi^*(N^\wedge N)$) emission upon excitation. The interactions of the complexes with avidin are studied by the HABA assay and emission titrations. The occurrence of the equivalence points at [Ir]:[avidin] = 2 indicates that the two biotin moieties of the same complex can bind to avidin ($K_d = 7.5 \times 10^{-9}$ to 1.8×10^{-8} M). Also, emission enhancement (1.2- to 2.3-fold) is observed when avidin is added to the complexes. The possibility of these luminescent complexes as cross-linkers for avidin is examined by RET-based emission quenching experiments, microscopy studies using avidin-conjugated microspheres and HPLC analysis. The results show that avidin-dimers and -trimers are formed and the avidin-crosslinking properties of complexes depend on the distance between the two biotin moieties in each complex and the direction constraint exerted by the $[Ir(N^\wedge C)_2]$ unit. In another study, three bis-biotin complexes $[Ir(N^\wedge C)_2(N^\wedge N)]^+$ (HN^C = Hppy-4-CH_2-NH-C6-NH-biotin, N^N = bpy; HN^C = Hppy, N^N = bpy-CONH-C2-NH-biotin2; HN^C = Hppy, N^N = bpy-CONH-C2-NHCO-C6-NH-biotin2) and one tris-biotin complex $[Ir(ppy\text{-}4\text{-}CH_2\text{-}NH\text{-}C6\text{-}NH\text{-}biotin)_2(bpy\text{-}CONH\text{-}C6\text{-}NH\text{-}biotin)]^+$ and their biotin-free counterpart $[Ir(ppy)_2(bpy\text{-}C4)]^+$ (**42**) are reported [61]. All the complexes display intense and long-lived orange-yellow to red triplet metal-to-ligand charge-transfer (^{3}MLCT) ($d\pi(Ir) \rightarrow \pi^*(N^\wedge N)$) emission upon irradiation. The interactions of the bis-biotin and tris-biotin complexes with avidin are studied by HABA assays, emission titrations and dissociation assays. In HABA assays, the equivalence point for the tris-biotin complex appears at [Ir]:[avidin] = ca. 1.6, which is larger than the ideal value 4/3. Emission titration results reveal that the complexes, in which the two biotin moieties are appended to the cyclometallating ligand, exhibit larger emission enhancement factors (1.8–2.5) than the complex that contain two biotin moieties in the ppy ligands. The off-rate constants k_{off} were determined from dissociation assays and ranged from 2.0×10^{-4} to 6.5×10^{-3} s^{-1}. The avidin-crosslinking properties of these complexes are confirmed by the results that (a) agglomeration of avidin-modified microspheres occurs upon addition of the biotin complexes and (b) the peaks corresponding to the avidin dimer, trimer and even polymer are observed in the chromatograms of a mixture of avidin and the biotin complex. Selected results are summarised in Fig. 8. Utilisation of these luminescent iridium(III) biotin complexes in signal amplification is demonstrated using avidin-coated non-fluorescent microspheres. Successive incubation of avidin-coated non-fluorescent microspheres with one of the bis-biotin complexes and avidin is performed, with stringent washing between each incubation step. After immobilisation of five layers of the complex, the average emission intensity of the microspheres is ca. 18 times higher than that immobilised with just one layer of complex. Similar results are not obtained when BSA is used instead of avidin or when the avidin is presaturated with biotin from the onset, indicating that the increasing emission intensity relies on the emission and avidin-crosslinking properties of the complex.

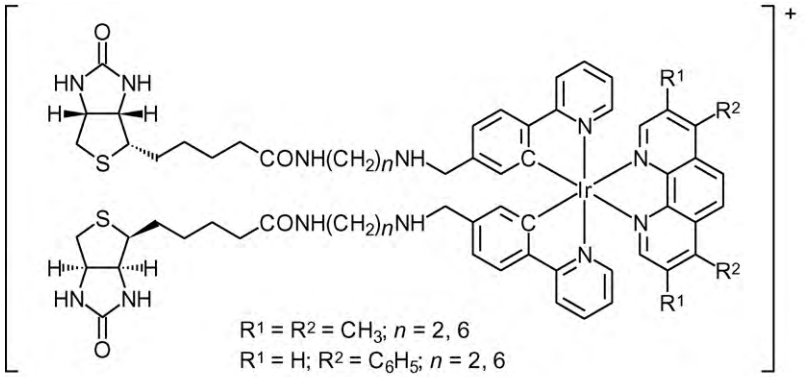

41

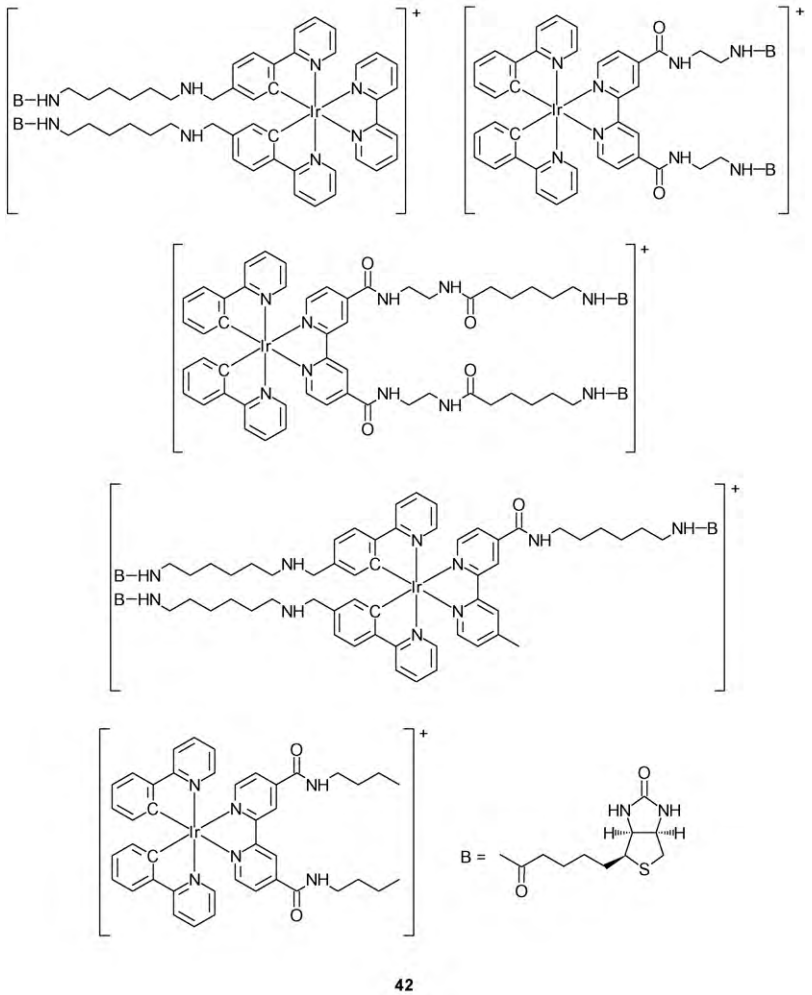

42

Hong and co-workers reported a neutral tripod complex (**43**), which consists of an energy acceptor (FIrpic), an energy donor (mCP) and biotin [62]. The luminescence of this complex results from both ^{1}MLCT ($d\pi(Ir) \rightarrow \pi^*(N\hat{}O)$) and ^{3}IL in the FIrpic moiety and shows a similar emission spectrum (λ_{max} = 472 nm) to that of FIrpic. The good overlap between the emission spectrum of the donor (mCP unit) and the absorption spectrum of FIrpic over 350 nm (^{1}MLCT and ^{3}IL region) ensures singlet–singlet energy transfer from mCP to FIrpic. Upon binding to avidin, the complex shows a large increase in emission intensity (ca. 14-fold) when excited at the donor absorption peak (310 nm). In contrast, the donor-free complex only shows a 1.6-fold increase in the emission intensity upon binding to avidin, indicating that intramolecular energy transfer can be an effective method for increasing the sensitivity.

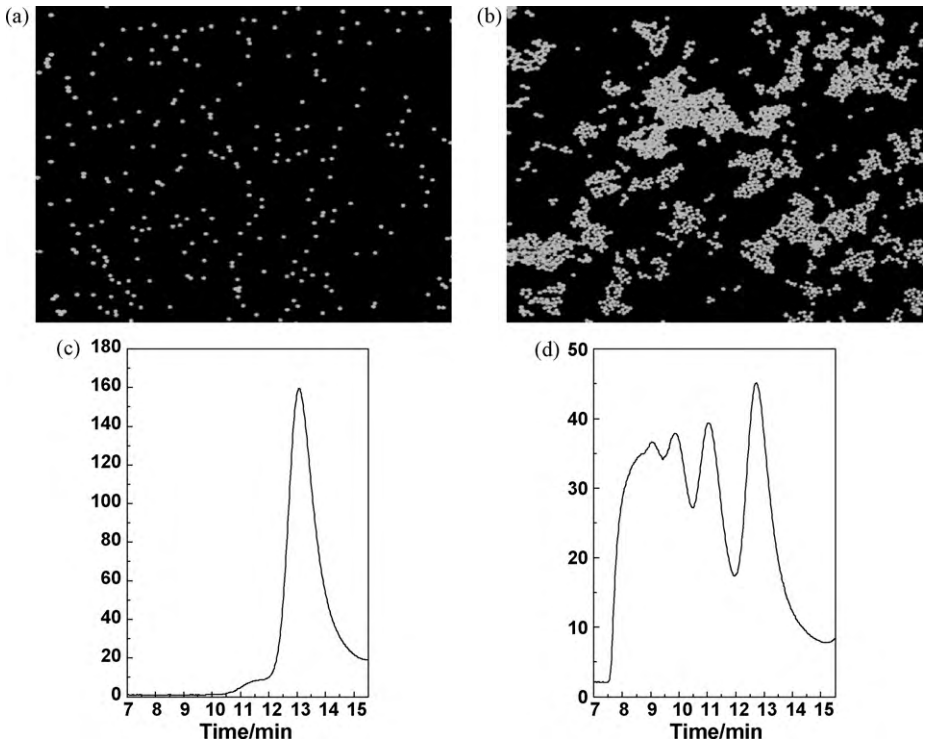

Fig. 8. Confocal microscopy images of avidin-modified fluorescent microsphere suspensions containing iridium(III) (a) mono-biotin and (b) tris-biotin complexes, respectively. Size-exclusion chromatograms of an equimolar mixture of 0.12 mM avidin and iridium(III) (c) mono-biotin and (d) tris-biotin complexes, respectively, in 50 mM potassium phosphate buffer, pH 7.4.

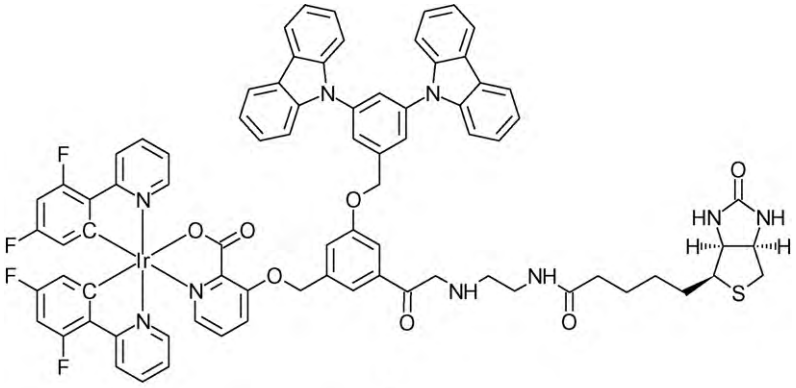

43

Most of probes derived from luminescent iridium(III) complexes display changes in their emission intensities and lifetimes upon analyte binding. Although in some cases the emission maxima exhibit small shifts, the emission profiles and spectral characteristics of the luminescent probes basically remain the same. Recently, Lo et al. reported a cyclometallated iridium(III) polypyridine complex $[Ir(ppy\text{-}4\text{-}CH_2\text{-}NH\text{-}C_4H_9)_2(bpy\text{-}CONH\text{-}C_2H_5)]^+$ (**44**), which shows interesting dual emission in fluid solutions at room temperature [63]. The complex displays a high-energy (HE) structured band at ca. 500 nm (τ_o = 1.1–2.5 μs) and a low-energy (LE) broad band/shoulder at ca. 593–619 nm (τ_o = 0.1–0.3 μs). In degassed nonpolar solvents such as CH_2Cl_2, the emission intensity of the LE band is higher than or comparable to that of the HE band, while in more polar solvents such as CH_3CN and MeOH, it becomes much weaker; in aqueous buffer the spectrum is dominated by the HE band (Fig. 9a). On the basis of the spectral profiles, emission wavelengths and lifetimes, the HE and LE emission bands are assigned to ^{3}IL ($\pi \rightarrow \pi^*$) (N^N or N^C) and ^{3}CT ($d\pi(Ir)/\pi(N^C)/amine \rightarrow \pi^*(N^N)$) excited states, respectively. Based on these interesting environment-sensitive emission properties, a series of dual-emissive iridium(III) complexes $[Ir(ppy\text{-}4\text{-}CH_2\text{-}NH\text{-}C_4H_9)_2(N^N)]^+$ (N^N = bpy-CONH-C6-NH-biotin, bpy-CONH-C6-Ph-est, bpy-CONH-$C_{18}H_{37}$), containing a biotin, an estradiol and a hydrophobic C18 chain, respectively, are designed as protein probes. The biotin complex exhibits one structured HE band at ca. 492 nm in aerated buffer. Remarkably, in the presence of avidin, the HE emission band displays a 52% decrease in intensity (τ increased from 0.54 to 0.91 μs) while a new LE shoulder at about 608 nm (τ = 66 ns) appears in the spectrum, resulting in a sharp isoemissive point at ca. 574 nm (Fig. 9b). The estradiol complex shows similar dual-emissive properties. In aerated buffer, it displays a structured HE band at ca. 496 nm and an LE band of comparable intensity at ca. 580 nm due to the hydrophobic estradiol group. Upon addition of ERα, the LE band shows a ca. 3.3-fold increase in the emission intensity (Fig. 9c). The lifetimes of the HE and LE bands increase from 0.63 μs and 56 ns to 0.84 μs and 0.21 μs, respectively. Similar to the estradiol complex, the C18 complex in aerated buffer displays an LE emission band at about 593 nm

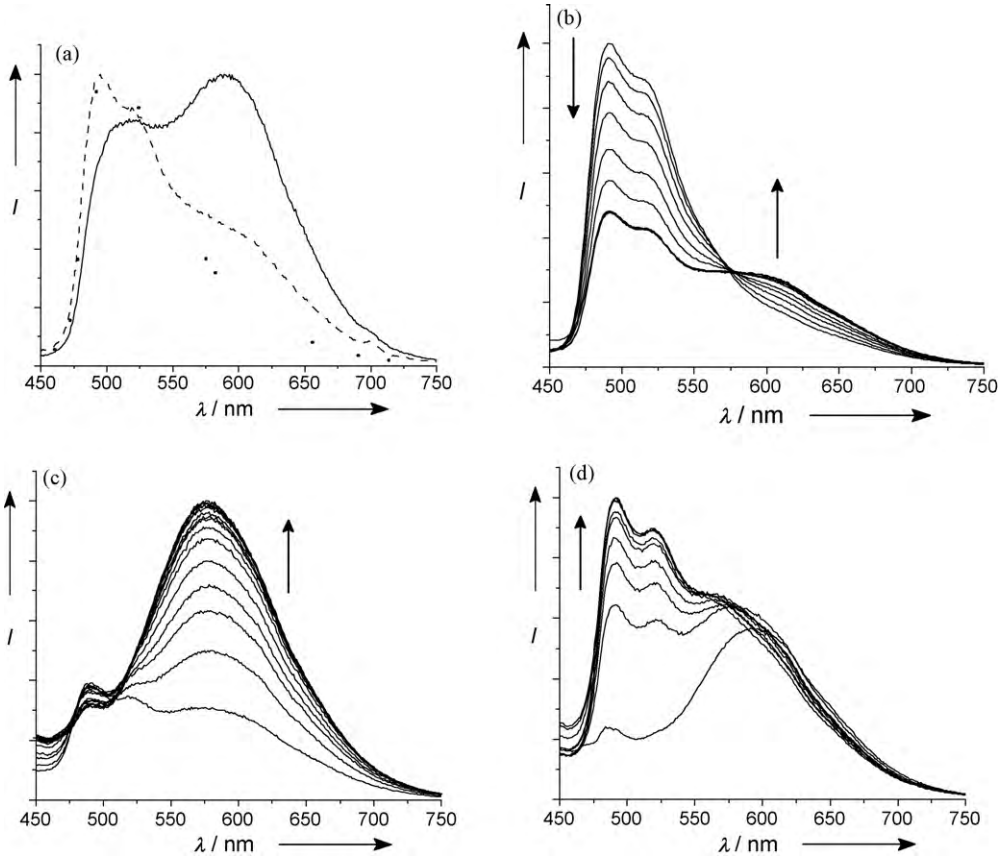

Fig. 9. (a) Normalised emission spectra of $[Ir(ppy\text{-}4\text{-}CH_2\text{-}NH\text{-}C_4H_9)_2(bpy\text{-}CONH\text{-}C_2H_5)]^+$ in degassed CH_2Cl_2 (solid line), CH_3CN (dashed line) and phosphate buffer (dotted line) at 298 K. Emission spectral traces of (b) $[Ir(ppy\text{-}4\text{-}CH_2\text{-}NH\text{-}C_4H_9)_2(bpy\text{-}CONH\text{-}C6\text{-}NH\text{-}biotin)]^+$, (c) $[Ir(ppy\text{-}4\text{-}CH_2\text{-}NH\text{-}C_4H_9)_2(bpy\text{-}CONH\text{-}C6\text{-}Ph\text{-}est)]^+$ and (d) $[Ir(ppy\text{-}4\text{-}CH_2\text{-}NH\text{-}C_4H_9)_2(bpy\text{-}CONH\text{-}C_{18}H_{37})]^+$ in aerated phosphate buffer at 298 K upon addition of avidin, ERα and HSA, respectively.

(τ_o = 0.12 μs), whose intensity is even higher than that of the HE band (τ_o = 0.55 μs). This LE emission feature is attributed to the wrapping of the complex by the very hydrophobic octadecyl chain in the highly polar buffer medium. Upon addition of a lipid-binding protein HSA, the intensity of the HE emission band at ca. 492 nm increases by ca. 4.4-fold (τ = 1.22 μs), whereas the LE emission band does not show any difference and eventually becomes a shoulder at ca. 576 nm (τ = 0.19 μs) (Fig. 9d). It is likely that the octadecyl chain binds to the hydrophobic lipid-binding cavity of the protein, thereby increasing the exposure of the iridium(III) polypyridine to the polar buffer and leading to the predominant HE emission. Interestingly, a similar emission profile (I_{HE}/I_{LE} = ca. 1.3:1) is observed when β-CD, which binds long aliphatic chains strongly, is added to an aerated solution of the complex in buffer. Additionally, vesicles prepared from DSPC and the C18 complex exhibit strong orange-yellow emission as a result of a strong LE band at ca. 587 nm in degassed buffer, which is in sharp contrast to the green emission of the complex (λ_{em} = 494 nm) in degassed buffer without the vesicles. These observations indicate that the C18 complex is localised in the hydrophobic region of the vesicles and would serve as an excellent probe for lipid bilayers, micelles and lipoproteins.

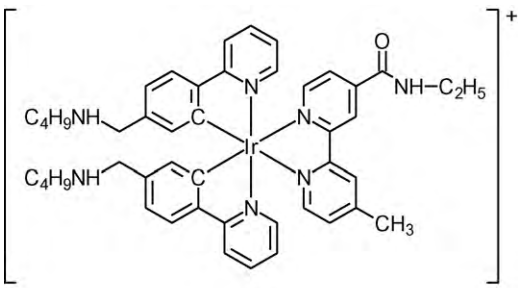

44

3.4. Cellular probes

Li and co-workers demonstrated two cationic iridium(III) complexes $[Ir(dfpy)_2(N^N)]^+$ (N^N = bpy, quqo) (**45**), displaying bright green and red emission, respectively, as phosphorescent dyes for live cell imaging [64]. HeLa cells treated with these complexes

show the exclusive staining in cytoplasm, making the complexes promising candidates for the design of specific phosphorescence bioimaging agents.

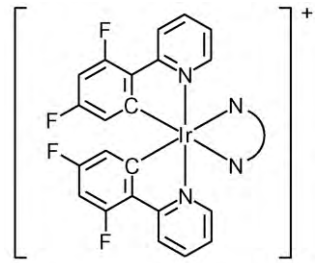

45

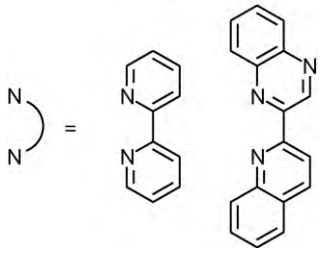

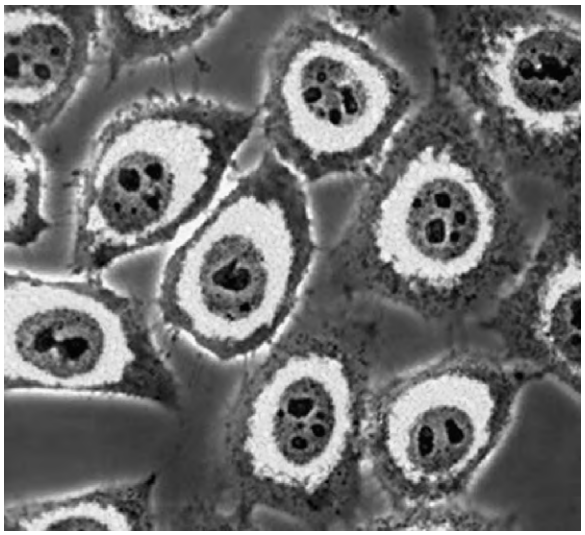

Fig. 10. Confocal and brightfield overlaid microscopy images of HeLa cells incubated with $[Ir(pq)_2(bpy\text{-}spacer\text{-}indole)]^+$ (5 μM) at 37 °C for 1 h.

Lo and co-workers studied the lipophilicity, cytotoxicity and cellular uptake properties of iridium(III) indole (**37**) [55] and biotin (**42**) [61] complexes and their substrate-free counterparts towards HeLa cells by reversed-phase HPLC, the MTT assay and flow cytometry and laser-scanning confocal microscopy, respectively. The lipophilicity closely relates to the ability of a cellular probe and reagent to permeate biological membranes and is commonly estimated by the partition coefficient ($P_{o/w}$) in *n*-octanol/water. The $P_{o/w}$ values of the indole complexes, biotin complexes and substrate-free complex range from 1.30–3.40, 1.34–2.83 and 0.44–3.40, respectively. In addition, the log $P_{o/w}$ values of the complexes follow the order: ppy < bzq < pq, which is in accordance with the hydrophobic character of the ligands. Interestingly, the indole moiety renders the complexes more lipophilic and the biotin moiety leads to the opposite, indicating the lipophilic and hydrophilic of indole and biotin, respectively. The IC_{50} values are determined from the dose dependence of surviving HeLa cells after their exposure to the complexes for 48 h. The IC_{50} values, obtained from the MTT assays, of the indole complexes range from 1.1 to 6.3 μM, which are comparable to the substrate-free complex (IC_{50} value = 3.2 μM) and significantly smaller than that of cisplatin (30.7 μM) under the same experimental conditions. In contrast, the biotin complexes are basically noncytotoxic (IC_{50} values > 400 μM). The microscopy images show that indole complexes are localised in the perinuclear region upon internalisation (Fig. 10). Temperature-dependence experiments suggest that the uptake of the complex is an energy-requiring process such as endocytosis. In the case of the biotin complexes, emissive cytoplasmic granules are observed, which may result from endosomal labelling and/or aggregation of the luminescent complexes. Importantly, HeLa cells loaded with the substrate-free complex reveal much more intense emission. It is interesting to note that this complex forms a diffuse background in addition to cytoplasmic granules that are also observed in the biotin complexes, indicative of the endocytic uptake, as well as the passive diffusion of the complex.

The same group reported a series of new luminescent iridium(III) polypyridine complexes $[Ir(N^{\wedge}C)_2(N^{\wedge}N)]^+$ (HN^C = Hppy, Hppz, Hpq; N^N = bpy-CONH-$C_{18}H_{37}$, bpy-CONH-$C_{10}H_{21}$, bpy-CONH-C_2H_5) (**46**) bearing an alkyl pendant [65]. Upon irradiation, all the complexes exhibited intense and long-lived ^{3}MLCT ($d\pi(Ir) \rightarrow \pi^*(N^{\wedge}N)$) luminescence in homogeneous fluid solutions at 298 K and in alcohol glass at 77 K. The emissive states of the pq complexes are probably mixed with some ^{3}IL ($\pi \rightarrow \pi^*$) (pq) character. All the complexes are incorporated into phospholipid vesicles composed of DSPC, and these vesicles are strongly emissive in aqueous solution. The cryo-TEM images of Ir/DSPC liposomes show the existence of polygonal vesicles, the majority of which had a diameter between 20 and 140 nm. The lipophilicity (log $P_{o/w}$ values) of the complexes ranged from −0.34 to 9.89 and follows the order ppz < ppy < pq and C2 < C10 < C18, which is in accordance with the hydrophobic character of the ligands. Cytotoxicity studies reveal that the C10 complexes exhibited the highest cytotoxicity among the complexes studied, with the IC_{50} values being almost 10 times lower than that of cisplatin. The IC_{50} values of the C18 complexes are comparable to those of the C2 complexes. The cellular uptake characteristics of the complexes have been investigated using flow cytometry. The emission intensities of the cells treated with the pq complexes follow the order C10 > C2 > C18. Since (i) the emission wavelengths and intensities of the pq complexes are comparable, (ii) the responses of the complexes towards hydrophobic micellar media are similar and (iii) the complexes are localised in a similar region in the cells, the trend observed in the flow cytometric measurements can be correlated to the cellular uptake efficiencies of the complexes. Thus, these results illustrate that although efficient internalisation of the complexes is supposed to be assisted by their high lipophilicity, C18, being the most lipophilic complex among the three, shows the lowest cellular uptake efficiency. This could be due to its largest molecular size or possible self-aggregation. Live cell confocal images show that most of the complex molecules are distributed inside the cytoplasm with a lower extent of nuclear uptake, as revealed by the much more weakly stained nucleus. A higher degree of localisation of the complexes in the perinuclear region is likely to result from the interactions of the complex molecules with hydrophobic organelles such as endoplasmic reticulum, mitochondria and Golgi apparatus. When the cells are incubated at 4 °C, no interiorisation is observed, implying that the uptake of the complex and its subsequent localisation are due to energy-requiring processes such as endocytosis.

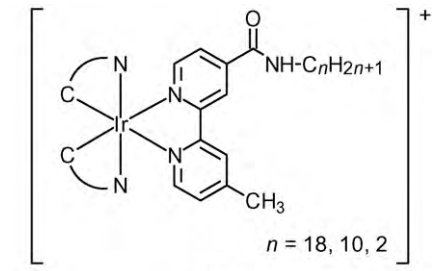

46

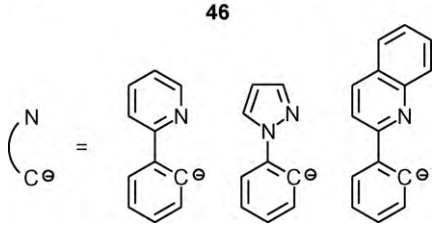

4. Concluding remarks

The use of luminescent rhenium(I) and iridium(III) complexes as probes for ions, molecules and biomolecules has been reviewed in this article. Early development of sensory systems with luminescent transition metal complexes was focused on ruthenium(II) polypyridine complexes. However, it can be seen in this review that the intriguing emissive behaviour of rhenium(I) and iridium(III) polypyridine complexes has been utilised in sensing applications. The diverse structural, spectroscopic and emission properties of these complexes mean that they are very promising candidates as probes for a wide range of ions and molecules. With more understanding on the emission–electronic structure relationships, as revealed by theoretical calculations, as well as the knowledge on the interactions of these complexes with simple ions and molecules, there is a recent trend in using these complexes for probing more complex biological systems; for example, reports on the development of sensors imaging reagents and cellular probes have started to appear. In conclusion, we anticipate that the interesting structural and emissive properties of rhenium(I) and iridium(III) complexes will continue to contribute to the development of sensitive and selective sensory systems.

Acknowledgements

We thank the Hong Kong Research Grants Council (Project Numbers CityU 101908 and CityU 102109) for financial support. MWL and KYZ acknowledge the receipt of a Postgraduate Studentship, a Research Tuition Scholarship and Outstanding Academic Performance Award, all administered by the City University of Hong Kong. I am very grateful to members of my research group and to my collaborators, all of whose names appear on the reference list.

References

[1] M.S. Wrighton, D.L. Morse, J. Am. Chem. Soc. 96 (1974) 998.
[2] A.J. Lees, Chem. Rev. 87 (1987) 711.
[3] V. Balzani, F. Scandola, Supramolecular Photochemistry, Ellis Horwood, New York, 1990.
[4] K. Kalyanasundaram, Photochemistry of Polypyridine and Porphyrin Complexes, Academic Press, San Diego, 1992.
[5] D.M. Roundhill, Photochemistry and Photophysics of Metal Complexes, Plenum Press, New York, 1994.
[6] D.J. Stufkens, A. Vlček Jr., Coord. Chem. Rev. 177 (1998) 127.
[7] A.I. Baba, J.R. Shaw, J.A. Simon, R.P. Thummel, R.H. Schmehl, Coord. Chem. Rev. 171 (1998) 43.
[8] S.C. Rasmussen, M.M. Richter, E. Yi, H. Place, K.J. Brewer, Inorg. Chem. 29 (1990) 3926.
[9] I.M. Dixon, J.-P. Collin, J.-P. Sauvage, L. Flamigni, S. Encinas, F. Barigelletti, Chem. Soc. Rev. 29 (2000) 385.
[10] J.A.G. Williams, A.J. Wilkinson, V.L. Whittle, Dalton Trans. (2008) 2081.
[11] V.W.-W. Yam, K.M.-C. Wong, V.W.-M. Lee, K.K.-W. Lo, K.-K. Cheung, Organometallics 14 (1995) 4034.
[12] Y. Shen, B.P. Sullivan, Inorg. Chem. 34 (1995) 6235.
[13] S.S. Sun, A.J. Lees, Chem. Commun. (2000) 1687.
[14] M.-J. Li, W.-M. Kwok, W.-H. Lam, C.-H. Tao, V.W.-W. Yam, D.-L. Phillips, Organometallics 28 (2009) 1620.
[15] L.H. Uppadine, J.E. Redman, S.W. Dent, M.G.B. Drew, P.D. Beer, Inorg. Chem. 40 (2001) 2860.
[16] S.S. Sun, A.J. Lees, J. Am. Chem. Soc. 122 (2000) 8956.
[17] H.D. Stoeffler, N.B. Thornton, S.L. Temkin, K.S. Schanze, J. Am. Chem. Soc. 117 (1995) 7119.
[18] V.W.-W. Yam, K.K.-W. Lo, K.-K. Cheung, R.Y.-C. Kong, J. Chem. Soc., Chem. Commun. (1995) 1191.
[19] V.W.-W. Yam, K.K.-W. Lo, K.-K. Cheung, R.Y.-C. Kong, J. Chem. Soc., Dalton Trans. (1997) 2067.
[20] C. Metcalfe, M. Webb, J.A. Thomas, Chem. Commun. (2002) 2026.
[21] S.P. Foxon, T. Phillips, M.R. Gill, M. Towrie, A.W. Parker, M. Webb, J.A. Thomas, Angew. Chem. Int. Ed. 46 (2007) 3686.
[22] A.R. Dunn, W. Benlliston-Bittner, J.R. Winkler, E.D. Getzoff, D.J. Stuehr, H.B. Gray, J. Am. Chem. Soc. 127 (2005) 5169.
[23] X.Q. Guo, F.N. Castellano, L. Li, H. Szmacinski, J.R. Lakowicz, J. Sipior, Anal. Biochem. 254 (1997) 179.
[24] J.D. Dattelbaum, O.O. Abugo, J.R. Lakowicz, Bioconjugate Chem. 11 (2000) 553.
[25] K.K.-W. Lo, D.C.-M. Ng, W.-K. Hui, K.-K. Cheung, J. Chem. Soc., Dalton Trans. (2001) 2634.
[26] K.K.-W. Lo, W.-K. Hui, D.C.-M. Ng, K.-K. Cheung, Inorg. Chem. 41 (2002) 40.
[27] N.M. Green, Methods Enzymol. 184 (1990) 51.
[28] H.J. Gruber, M. Marek, H. Schindler, K. Kaiser, Bioconjugate Chem. 8 (1997) 552.
[29] K.K.-W. Lo, W.-K. Hui, D.C.-M. Ng, J. Am. Chem. Soc. 124 (2002) 9344.
[30] K.K.-W. Lo, K.H.-K. Tsang, Organometallics 23 (2004) 3062.
[31] K.K.-W. Lo, W.-K. Hui, Inorg. Chem. 44 (2005) 1992.
[32] K.K.-W. Lo, K.H.-K. Tsang, K.-S. Sze, Inorg. Chem. 45 (2006) 1714.
[33] K.K.-W. Lo, K.H.-K. Tsang, W.-K. Hui, N. Zhu, Chem. Commun. (2003) 2704.
[34] K.K.-W. Lo, K.H.-K. Tsang, W.-K. Hui, N. Zhu, Inorg. Chem. 44 (2005) 6100.
[35] K.K.-W. Lo, K.-S. Sze, K.H.-K. Tsang, N. Zhu, Organometallics 26 (2007) 3440.
[36] K.K.-W. Lo, K.H.-K. Tsang, N. Zhu, Organometallics 25 (2006) 3220.
[37] A.J. Amoroso, M.P. Coogan, J.E. Dunne, V. Fernández-Moreira, J.B. Hess, A.J. Hayes, D. Lloyd, C. Millet, S.J.A. Pope, C. Williams, Chem. Commun. (2007) 3066.
[38] S.L. Poynton, W. Fraser, R. Francis-Floyd, P. Rutledge, P. Reed, T.A. Nerad, J. Eukaryot. Microbiol. 42 (1995) 731.
[39] K.A. Stephenson, S.R. Banerjee, T. Besanger, O.O. Sogbein, M.K. Levadala, N. McFarlane, J.A. Lemon, D.R. Boreham, K.P. Maresca, J.D. Brennan, J.W. Babich, J. Zubieta, J.F. Valliant, J. Am. Chem. Soc. 126 (2004) 8598.
[40] K.K.-W. Lo, M.-W. Louie, K.-S. Sze, J.S.-Y. Lau, Inorg. Chem. 47 (2008) 602.
[41] M.-W. Louie, M.H.-C. Lam, K.K.-W. Lo, Eur. J. Inorg. Chem. (2009) 4265.
[42] M.-W. Louie, H.-W. Liu, M.H.-C. Lam, T.-C. Lau, K.K.-W. Lo, Organometallics 28 (2009) 4297.
[43] Q. Zhao, S. Liu, M. Shi, F. Li, H. Jing, T. Yi, C. Huang, Organometallics 26 (2007) 5922.
[44] H. Chen, Q. Zhao, Y. Wu, F. Li, H. Yang, T. Yi, C. Huang, Inorg. Chem. 46 (2007) 11075.
[45] Q. Zhao, F. Li, S. Liu, M. Yu, Z. Liu, T. Yi, C. Huang, Inorg. Chem. 47 (2008) 9256.
[46] W. Goodall, J.A.G. Williams, J. Chem. Soc., Dalton Trans. (2000) 2893.
[47] K.J. Arm, W. Leslie, J.A.G. Williams, Inorg. Chim. Acta 359 (2006) 1222.
[48] M.-L. Ho, F.-M. Hwang, P.-N. Chen, Y.-H. Hu, Y.-M. Cheng, K.-S. Chen, G.-H. Lee, Y. Chi, P.-T. Chou, Org. Biomol. Chem. 4 (2006) 98.
[49] K.K.-W. Lo, J.S.-Y. Lau, D.K.-K. Lo, L.T.-L. Lo, Eur. J. Inorg. Chem. (2006) 4054.
[50] K.K.-W. Lo, C.-K. Chung, N. Zhu, Chem. Eur. J. 12 (2006) 1500.
[51] C. Stinner, M.D. Wightman, S.O. Kelley, M.G. Hill, J.K. Barton, Inorg. Chem. 40 (2001) 5245.
[52] F. Shao, B. Elias, W. Lu, J.K. Barton, Inorg. Chem. 46 (2007) 10187.
[53] D.-L. Ma, W.-L. Wong, W.-H. Chung, F.-Y. Chan, P.-K. So, T.-S. Lai, Z.-Y. Zhou, Y.-C. Leung, K.-Y. Wong, Angew. Chem. Int. Ed. 47 (2008) 3735.
[54] K.K.-W. Lo, K.Y. Zhang, C.-K. Chung, K.Y. Kwok, Chem. Eur. J. 13 (2007) 7110.
[55] J.S.-Y. Lau, P.-K. Lee, K.H.-K. Tsang, C.H.-C. Ng, Y.-W. Lam, S.-H. Cheng, K.K.-W. Lo, Inorg. Chem. 48 (2009) 708.
[56] K.K.-W. Lo, J.S.-W. Chan, L.-H. Lui, C.-K. Chung, Organometallics 23 (2004) 3108.
[57] K.K.-W. Lo, C.-K. Li, J.S.-Y. Lau, Organometallics 24 (2005) 4594.
[58] D.S. Wilbur, P.M. Pathare, D.K. Hamlin, S.A. Weerawarna, Bioconjugate Chem. 8 (1997) 819.
[59] D.S. Wilbur, P.M. Pathare, D.K. Hamlin, K.R. Buhler, R.L. Vessella, Bioconjugate Chem. 9 (1998) 813.
[60] K.K.-W. Lo, J.S.-Y. Lau, Inorg. Chem. 46 (2007) 700.
[61] K.Y. Zhang, K.K.-W. Lo, Inorg. Chem. 48 (2009) 6011.
[62] T.-H. Kwon, J. Kwon, J.-I. Hong, J. Am. Chem. Soc. 130 (2008) 3726.
[63] K.K.-W. Lo, K.Y. Zhang, S.-K. Leung, M.-C. Tang, Angew. Chem. Int. Ed. 47 (2008) 2213.
[64] M. Yu, Q. Zhao, L. Shi, F. Li, Z. Zhou, H. Yang, T. Yi, C. Huang, Chem. Commun. (2008) 2115.
[65] K.K.-W. Lo, P.-K. Lee, J.S.-Y. Lau, Organometallics 27 (2008) 2998.